Accepted Manuscript

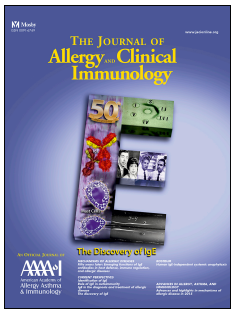

Human CD40L-expressing type 3 innate lymphoid cells induce IL-10-producing immature transitional regulatory B cells

Zsolt István Komlósi, MD, PhD, Nóra Kovács, MD, Willem van de Veen, PhD, Anna Kirsch, MD, Heinz Benedikt Fahrner, MD, Marcin Wawrzyniak, PhD, Ana Rebane, PhD, Barbara Stanic, PhD, Oscar Palomares, PhD, Beate Rückert, MSc, Günter Menz, MD, Mübeccel Akdis, MD, PhD, György Losonczy, MD, DSc, Cezmi A. Akdis, MD

PII: S0091-6749(17)31460-4

DOI: 10.1016/j.jaci.2017.07.046

Reference: YMAI 13010

To appear in: *Journal of Allergy and Clinical Immunology*

Received Date: 6 December 2016

Revised Date: 18 June 2017

Accepted Date: 13 July 2017

Please cite this article as: Komlósi ZI, Kovács N, van de Veen W, Kirsch A, Fahrner HB, Wawrzyniak M, Rebane A, Stanic B, Palomares O, Rückert B, Menz G, Akdis M, Losonczy G, Akdis CA, Human CD40L-expressing type 3 innate lymphoid cells induce IL-10-producing immature transitional regulatory B cells, *Journal of Allergy and Clinical Immunology* (2017), doi: 10.1016/j.jaci.2017.07.046.

Human CD40L-expressing type 3 innate lymphoid cells induce IL-10-producing immature transitional regulatory B cells

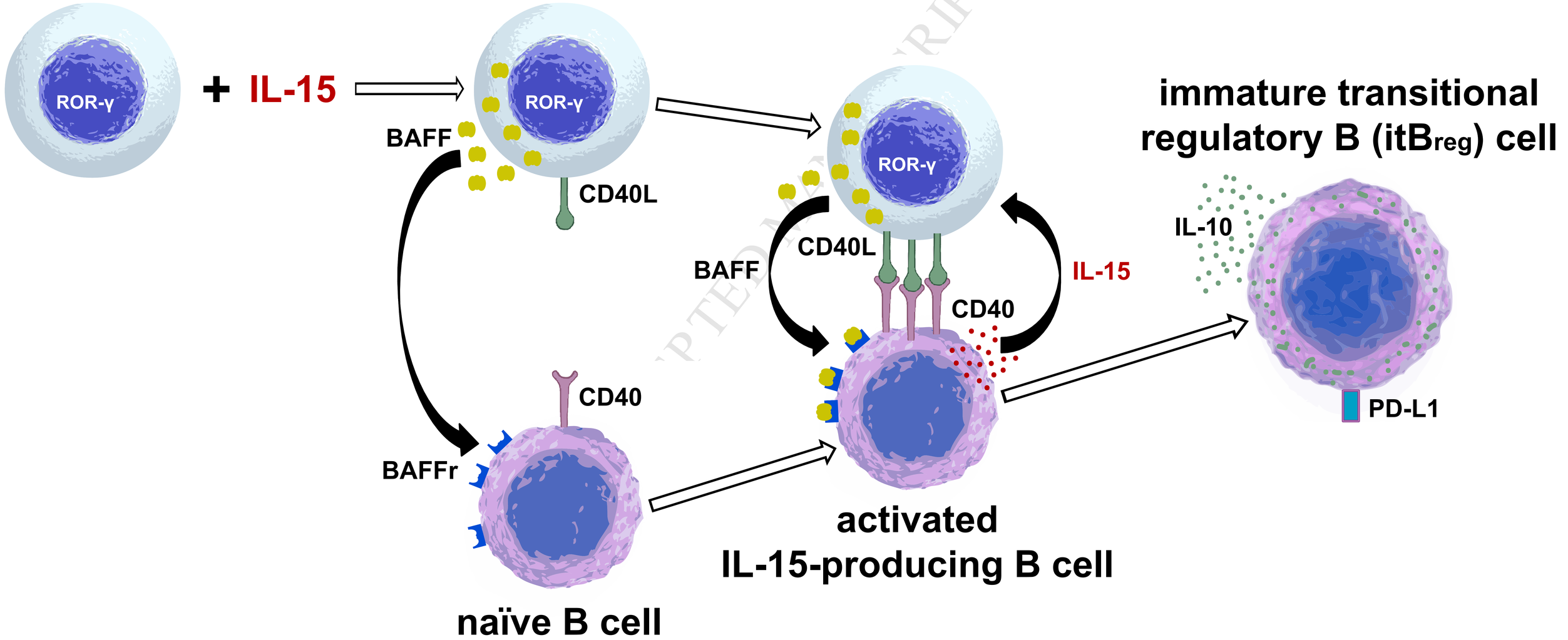

Human CD40L-expressing type 3 innate lymphoid cells induce IL-10-producing immature transitional regulatory B cells

Zsolt István Komlósi, MD, PhD,[1,2]*, Nóra Kovács, MD, [1,3], Willem van de Veen, PhD, [1], Anna Kirsch, MD, [4], Heinz Benedikt Fahrner, MD, [5], Marcin Wawrzyniak, PhD, [1], Ana Rebane, PhD, [1,6], Barbara Stanic, PhD, [1], Oscar Palomares, PhD, [1,7], Beate Rückert, MSc, [1], Günter Menz, MD, [4], Mübeccel Akdis, MD, PhD, [1], György Losonczy, MD, DSc, [2], Cezmi A. Akdis, MD, [1]*

Affiliations:

[1]Swiss Institute of Allergy and Asthma Research (SIAF), University of Zurich; CK-CARE: Christine Kühne Center for Allergy Research and Education, 7270 Davos, Switzerland.

[2]Semmelweis University, Department of Pulmonology, 1125 Budapest, Hungary.

[3]Lung Health Hospital, 2045 Törökbálint, Hungary.

[4]Hochgebirgsklinik, 7265 Davos-Wolfgang, Switzerland.

[5]Department of ENT, Kantonsspital Graubünden, 7000 Chur, Switzerland.

[6]Institute of Biomedicine and Translational Medicine, University of Tartu, 50411 Tartu, Estonia.

[7]Department of Biochemistry and Molecular Biology, School of Chemistry, Complutense University of Madrid, 28040 Madrid, Spain.

*Corresponding authors: Zsolt István Komlósi and Cezmi A. Akdis

Correspondence should be addressed:

Zsolt I. Komlósi MD PhD, Dept. of Pulmonology, Semmelweis University, 1/C Diosarok, 1125 Budapest, Hungary; Phone: +36203411204; Fax: +3612142498

e-mail: drkomlo@yahoo.com; komlosi.zsolt@med.semmelweis-univ.hu

ABSTRACT

Background: Type 3 innate lymphoid cells (ILC3s) are involved in the maintenance of mucosal homeostasis; however, their role in immunoregulation has been unknown. Immature transitional regulatory B (itB_{reg}) cells are innate-like B cells with immunosuppressive properties, and the *in vivo* mechanisms by which they are induced have not been fully clarified.

Objective: We aimed to investigate the ILC3-B cell interaction that probably takes place in human tonsils.

Methods: ILC3s were isolated from peripheral blood and palatine tonsils, expanded and cocultured with naïve B cells. Tonsillar ILC3s and B_{reg} cells were visualized with immunofluorescence histology. The frequencies of ILC3s were measured in tonsil tissue of allergic and non-allergic patients; and in peripheral blood of allergic asthmatics and healthy controls.

Results: A mutually beneficial relationship was revealed between ILC3s and B cells: ILC3s induced IL-15 production in B cells via BAFF-receptor, while IL-15, a potent growth factor for ILC3s, induced the expression of CD40L on circulating and tonsillar ILC3s. IL-15-activated $CD40L^+$ILC3s helped B cell survival, proliferation and the differentiation of IL-10-secreting, functional itB_{reg} cells in a CD40L- and BAFF-receptor-dependent manner. ILC3s and B_{reg} cells were in close connection with each other in palatine tonsils. The frequency of ILC3s was reduced in tonsil tissue of allergic patients and in peripheral blood of allergic asthmatics.

Conclusion: Human $CD40L^+$ILC3s provide innate B cell help, and are involved in an innate immunoregulatory mechanism by the induction of itB_{reg} cell differentiation, which takes place in palatine tonsils *in vivo*. This mechanism may contribute to the maintenance of the immune tolerance and become insufficient in allergic diseases.

KEY MESSAGES

- CD40L-expressing, activated ILC3s provide innate B cell help in tonsils, and induce IL-10-producing, PD-L1-expressing, functional B_{reg} cells with an immature transitional phenotype.
- ILC3s and B cells communicate with each other via CD40L, B cell-activating factor and IL-15.
- The frequency of ILC3s is reduced in tonsil tissue of allergic patients and in peripheral blood of allergic asthmatics.

CAPSULE SUMMARY

ILC3-mediated induction of B_{reg} cells is a novel, innate immunoregulatory mechanism that may contribute to the maintenance of immune tolerance and become insufficient in allergy, as the frequency of ILC3s is reduced in allergic diseases.

Key words: Type 3 innate lymphoid cells, ILC3, immature transitional regulatory B cells, B_{reg}, tonsils, allergy, asthma, IL-10, immunoregulation, immune tolerance.

Abbreviations: APRIL, a proliferation-inducing ligand; BAFF, B cell-activating factor; BAFFr, BAFF-receptor; B_{reg} cell, regulatory B cell; cNK cell, conventional NK cell; GINA, Global Initiative for Asthma; ILC, innate lymphoid cell; ILC3, type 3 innate lymphoid cell; itB_{reg} cell, immature transitional regulatory B cell; L cell, human CD40L-expressing mouse fibroblast; mDC, myeloid dendritic cell; MFI, median fluorescence intensity; NK cell, natural killer cell; PBMC, peripheral blood mononuclear cell; PD-L1, programmed death-ligand 1; RORγt, Retinoic acid receptor-related orphan receptor-γt; SEM, standard error of the mean; TMC, tonsillar mononuclear cell; T_{reg} cell, regulatory T cell.

INTRODUCTION

The exploration of the diversity of innate lymphoid cells (ILCs)[1-2] and "innate-like" B cell subsets with regulatory potential[3] has substantially redrawn the picture of immune homeostasis and tissue inflammation. Despite detailed descriptions of the mechanisms by which ILC subsets contribute to various adaptive and innate immune processes[2, 4], their involvement in immunoregulation has not been delineated yet. Retinoic acid receptor-related orphan receptor-γt (RORγt)-expressing type 3 ILCs (ILC3s) in adult mice and humans play a role in the innate immune defense at the mucosal barrier surfaces[5] and tissue regeneration after damage[6-9]; mainly via secretion of their signature-cytokine IL-22[10-12]. ILC3s are also involved in limitation of pathological adaptive immune responses against commensal bacteria in the gut[13]. Thus, ILC3s have a dedicated role in maintenance and restoration of homeostasis at the interface of the environment and the body[4].

Among the several B cell subsets with immunoregulatory properties that have been identified[14], there is an immature transitional regulatory B (itB_{reg}) cell subpopulation with $CD19^{+}CD27^{-}IgD^{+}IgM^{+}CD24^{high}CD38^{high}CD1d^{high}$ phenotype and IL-10-producing capacity[15]. The *in vivo* differentiation pathway of itB_{reg} cells has not been fully explored so far[14].

It has recently been shown that ILCs can have an influence on antibody production in mice[16-17] and splenic ILC3s stimulate marginal zone B cells via CD40L (CD154) and B cell-activating factor (BAFF), and help to orchestrate innate-like IgM antibody production in humans[18], suggesting that a functional ILC-B cell interaction takes place *in vivo*.

The present study describes that $CD40L^{+}$ILC3s reside on the border of the T cell - B cell areas in tonsils, and are in close contact with B cells *in vivo*. $CD40L^{+}$ILC3s and B cells are in mutually beneficial relationship with each other, as $CD40L^{+}$ILC3s strongly support survival and proliferation of the B cells, promote IgM secretion and IL-10-producing, programmed death-ligand 1 (PD-L1)-expressing itB_{reg} cell differentiation in a CD40L- and BAFF-dependent manner, while B cells upregulate IL-15, a growth factor for ILC3s, upon interaction with $CD40L^{+}$ILC3s. ILC3s may contribute to the maintenance of the immune

tolerance via induction of itB_{reg} cells. A relative deficiency of ILC3s in allergic diseases is demonstrated.

MATERIALS AND METHODS

Peripheral blood and tonsil tissue samples

Peripheral blood samples for *in vitro* cell culture experiments were collected from healthy volunteers.

Human palatine tonsil tissue samples of eight allergic and eleven non-allergic patients were obtained from hospitals of Davos and Chur, Switzerland. Patients underwent elective tonsillectomy because of hypertrophic and obstructive tonsils. Patients with clinical history of atopic dermatitis, food allergy or allergic asthma, together with skin prick test or specific IgE positivity were included in the allergic group. Only the samples of non-allergic patients were used for *in vitro* ILC3 and B cell coculture experiments. The prevalence of ILC3s and the *IL15* mRNA expression of the B cells upon *in vitro* stimulation were compared between samples of allergic and non-allergic donors. All donors were free of any current infection.

Forty-one adult, partly controlled, non-obese (BMI < 30), allergic eosinophilic asthma patients (Global Initiative for Asthma – GINA treatment Step 3 to 4) were included in the study at their arrival to the hospital (Hochgebirgsklinik, Davos-Wolfgang, Switzerland), before the introduction of any new medication, or starting of the rehabilitation program. The patients had atopy (positive skin prick test or specific IgE) and the asthma symptoms were related to the relevant allergen (e.g. exacerbated in pollen season; reduced in house dust mite free environment). All patients were on medium- or high-dose inhaled corticosteroid and long-acting β2-agonist treatment and have not received systemic glucocorticoids in last 4 month. Patients that fulfill these inclusion criteria were selected by a pulmonologist. Twenty-three age-matched healthy volunteers served as controls for comparison of circulating ILC3 levels. All sample preparation and analyses were performed within 3 hours of blood withdrawal. The leftover of the PBMC samples that were not used up for the experiments, were frozen and

stored in biobank. Therefore, altogether 17 healthy and 17 allergic asthmatic samples were available for the later performed itB_{reg} and T_{reg} cell measurements.

The study was approved by the Cantonal Ethics Committee *of Graubünden,* and informed consent was obtained from all donors.

Flow cytometry and cell sorting

Flow cytometry data were acquired on Galios (Beckman Coulter), FACS Aria II (Aria III upgrade) and LSRFortessa (Beckton Dickinson) instruments, and were analyzed with Kaluza software (Beckman Coulter). In order to improve the efficiency of ILC3 sorting, the peripheral blood mononuclear cell (PBMC) samples were first depleted of monocytes, T cells and B cells and TMC samples were depleted of B cells. For this purpose, the cells were labeled with magnetic microbead-bound anti-CD14, anti-CD3 and anti-CD19 antibodies (or just with anti-CD19 antibodies for TMCs) and the positive cell populations were depleted by immunomagnetic separation (AutoMACS, Miltenyi Biotec). We used the remaining cells for ILC3 sorting. Lineage markers (Lin) were CD3, CD19, CD20, CD14, CD34, CD11c, CD94 for ILC3 sorting experiments. Before naïve B cell sorting, monocytes and T cells were depleted from the samples. ILC3s and naïve B cells were sorted on a FACS Aria II instrument to high purity (≥98%).

Establishment of $CD40L^+$ILC3 cell line, as well as $CD40L^+$ILC3 and B cell cocultures

Sorted $Lin^-CD4^-CD56^-IL\text{-}7R\alpha^+CD161^+c\text{-}Kit^+$ ILC3s were expanded for 20 days with irradiated autologous PBMCs (30 Gy) and IL-15 (10 ng/mL). As IL-15 is a potent growth factor for conventional natural killer (cNK) cells[19] accordingly, CD94, a characteristic C-type lectin receptor of cNK cells was used to discriminate cNK cells from other ILCs. After expansion $CD94^-c\text{-}Kit^{high}CD40L^+$ ILC3s (referred to as $CD40L^+$ILC3s), as well as $CD94^-c\text{-}Kit^{high}CD40L^-$ ILC3s (referred to as $CD40L^-$ILC3s) and $CD94^+CD40L^-c\text{-}Kit^{low}$ cNK cells were sorted for *in vitro* experiments, including $CD40L^+$ILC3 and B cell, as well as $CD40L^-$ILC3 and B cell cocultures.

For the tonsil-derived and blood-derived coculture experiments $CD19^+CD27^-IgG^-IgA^-$ naïve B cells were sorted from a second blood sample of the same blood donor and another aliquot of the same TMC sample used for the initial ILC3 isolation, respectively.

In the coculture experiments all conditions ($CD40L^+$ILC3s alone, B cells alone, ILC3 + B cell cocultures, T + B cell cocultures and B + L cell cocultures) were initially stimulated with synthetic phosphorothioate B type CpG 2006 oligodeoxynucleotide (Microsynth; 1 µM) and cultured with IL-15 (10 ng/mL). $CD40L^+$ILC3s and B cells were cocultured in 1:1, 1:3, 1:7 and 1:15 ratios.

Statistical analysis

Data were analyzed in Statistica 7.0 and GraphPad Prism. Student's t-test or one-way analysis of variance (ANOVA) with Bonferroni *post hoc* test were used for parametric, and Mann–Whitney U test or Kruskal-Wallis test with Dunn's *post hoc* test were used for non-parametric variables, as appropriate. The interrelation of the various cell populations were analyzed by Spearman's rank correlation. Sample sizes were chosen based on previous studies. The only reason for data exclusion was the technical error of the cell culture. All results are expressed as means±SEM.

Further details of the methods are described in **Online Repository.**

RESULTS

Type 3 innate lymphoid cells of peripheral blood and tonsil tissue acquire CD40L-expression in response to IL-15

IL-15 is known to induce ILC proliferation[2, 20], however its role in ILC3 activation and differentiation has not been clear so far. Therefore, as a novel approach, we expanded ILC3s with IL-15 (for 20 days). Blood-derived ILC3s differentiated into 3 major cell populations upon IL-15 stimulation (**Fig 1, A**): $CD94^+CD40L^-c\text{-}Kit^{low}$ conventional natural killer (cNK) cells, $CD94^-CD40L^-c\text{-}Kit^{high}$ ILC3s (referred to as $CD40L^-$ILC3s) and $CD94^-CD40L^+c\text{-}Kit^{high}$ ILC3s

(referred to as CD40L$^+$ILC3s). Tonsillar ILC3s, however, had much less capacity to differentiate into cNK cells; whereas abundant CD40L$^-$ILC3, as well as CD40L$^+$ILC3 populations developed in these cultures (**Fig 1, B**).

ILC3s are CD45$^+$ cells of hematopoetic origin, consequently migrate from the bone marrow to secondary lymphoid organs and mucosa-associated lymphoid tissues through the blood-stream. ILC3s represent a rare cell subset both in the blood and in palatine tonsils (Non-allergic and Healthy groups in **Fig 8, B** and **C**, respectively). Lin$^-$CD4$^-$CD56$^-$IL-7Rα$^+$CD161$^+$c-Kit$^+$ ILC3s (**Fig E1, A and B**) were sorted and expanded for *in vitro* functional experiments. Freshly isolated ILC3s expressed high levels of *RORC* mRNA encoding RORγt, the signature transcription factor of the ILC3s (**Fig E1, C**).

Tonsillar epithelial cells and myeloid dendritic cells (mDCs) expressed high levels of *IL15* mRNA (**Fig 1, C**), they can be the local sources of this growth factor for ILC3s. Circulating ILC3s did not express natural killer receptor NKp44 (CD336) on their surface. Whereas primary tonsillar ILC3s were predominantly NKp44$^+$, blood-derived ILC3s acquired this mucosal phenotype in response to IL-15 (**Fig 1, D**).

In the next step, we aimed to determine the key characteristics of CD40L$^+$ILC3s in order to provide evidence that they are indeed in the ILC3 lineage. First, CD40L$^+$ILC3s expressed high level of *RORC* mRNA (**Fig 1, E**), as well as RORγt protein (**Fig 1, F**). Second, CD40L$^+$ILC3s secreted high amounts of IL-22 in response to IL-23 (**Fig 1, G**); and third, CD40L$^+$ILC3s did not express *GATA3* mRNA (**Fig E2, A**) or *TBX21* mRNA (encoding T-bet; **Fig E2, B**), representing the characteristic transcription factors of ILC2s and ILC1s, respectively[2]. In addition, tonsillar ILC3s expressed the mRNA encoding CD40L (*CD40LG*) directly after isolation of cells, without any culture (**Fig 1, H**) and CD40L protein was also shown on the surface of ILC3s *ex vivo* (**Fig 1, I**). CD40L$^+$ILC3s, did not express granzyme B or perforin, the characteristic cytotoxic enzymes of cNK cells (**Fig E2, C and D**).

CD40L$^+$ILC3s are residing at the interface between T cell and B cell areas in palatine tonsils and support B cell survival, proliferation and differentiation

Our next focus was to delineate the *in vivo* function of $CD40L^+$ILC3s. The anatomical localization of $CD40L^+$ILC3s in human palatine tonsils has implications on their functional properties. ILC3s typically reside in the interfollicular area in secondary lymphoid organs[13]. Besides Th17 cells, only ILC3s express RORγt in tonsil tissue. Therefore we visualized with immunofluorescence histology that $ROR\gamma t^+CD3^-$ ILC3s were particularly localized at the interface between T cell and B cell areas in tonsils; and were in close contact with $CD20^+$ B cells (**Fig E3**). CD40 is constitutively expressed on the surface of B lymphocytes. Its interaction with CD40L is crucial for the induction of B cell proliferation and differentiation, and also essential for their long term survival. CD40L-expressing $CD161^+$ ILCs were visualized with immunofluorescence histology, and were localized in the proximity of $CD20^+$ B cells in tonsils (**Fig E4**).

Considering the localization of the $CD40L^+$ILC3s in tonsils (**Fig E3**), it can be expected that the interaction of $CD40L^+$ILC3s and B cells takes place *in vivo*. $CD40L^+$ILC3s (as well as $CD40L^-$ILC3s) express toll-like receptor 9 (TLR9; **Fig E5, A**), thus, ILC3s and B cells[21] are both able to respond to unmethlyated CpG oligodeoxynucleotides. CD40L can be cleaved from the cell surface and released by $CD40L^+$ cells, such as activated T helper cells. The soluble form of CD40L (sCD40L) has similar B cell-stimulatory effect to membrane-bound CD40L[22]. $CD40L^+$ILC3s also released sCD40L, and this was further enhanced by CpG (**Fig E5, B**), while the surface expression of CD40L did not change in response to CpG stimulation (**Fig E5, C**).

In order to investigate ILC3-B cell interaction in detail, we cocultured $CD40L^+$ and $CD40L^-$ILC3s with B cells. We used autologous, $CD19^+CD27^-IgA^-IgG^-IgD^+IgM^+CD38^+$ naïve B cells of high purity (**Fig E6 A and B**). This B cell pool includes both immature transitional and mature naïve B cells[15, 23]. We demonstrated that both blood- and tonsil-derived $CD40L^+$ILC3s supported B cell survival and proliferation in a dose-dependent manner (**Fig 2, A-C** and **3, A and B**, respectively). IgM production was also strongly induced by $CD40L^+$ILC3s in cocultures. This effect was specifically attributable to ILC3s, as CD40L

stimulation solely, provided by L cells (irradiated, human CD40L-expressing mouse fibroblasts), was not sufficient to induce high IgM production (**Fig 2, D**).

CD40L$^+$ILC3-mediated innate B cell help is specifically focused on immature transitional B cells

The characterization of viable B cells in the cocultures demonstrated which subset is the preferred target of CD40L$^+$ILC3-mediated help. CD40L$^+$ILC3 and B cell cocultures were found to be considerably enriched in CD19$^+$CD27$^-$IgD$^+$IgM$^+$CD24^{high}CD38^{high}CD1d^{high} immature transitional B cells (itB cells defined in **Fig 4, A**). The itB cells were also proliferating in these cocultures, although slower than IgM single-positive B cells (**Fig 4, B**). In CD40L$^+$ILC3 cocultures, there was a small, but significant increase in the relative abundance of itB cells already on day 6 compared with CD40L$^-$ILC3 cocultures, L cell cocultures and B cells alone; and this difference became prominent on day 12 (**Fig 4, C**). CD40L$^+$ILC3s efficiently supported the long-term survival of itB cells, while L cells failed to exert the same effect. CD138$^+$ B cells were not detectable on day 12 in the CD40L$^+$ILC3 and B cell cocultures. In summary, these data demonstrate that CD40L$^+$ILC3s provided innate, T cell-independent help to itB cells. The presence of itB cells in tonsillar mononuclear cells (TMCs) was confirmed right after isolation, without any *in vitro* stimulation or cell culture (**Fig 4, D**).

CD40L$^+$ILC3s induce the development of IL-10-secreting PD-L1$^+$B$_{reg}$ cells

The secretion of IL-10, IL-1ra and IL-6 dose-dependently increased in parallel to the increasing proportion of CD40L$^+$ILC3s in B cell cocultures. The balance between regulatory (IL-10, IL-1ra) and pro-inflammatory (IL-6) cytokines remarkably tilted towards the regulatory direction in CD40L$^+$ILC3 and B cell cocultures, suggesting the development of B$_{reg}$ cells. In contrast, this balance rather skewed towards pro-inflammatory cytokine IL-6 in the cocultures of B cells and L cells (**Fig 5, A**). Our data clearly demonstrated that the IL-10-producing B cell differentiation was dose-dependently related to the relative abundance of CD40L$^+$ILC3s

in the blood-derived cocultures (**Fig 5, B**) and was efficiently induced in tonsil-derived CD40L$^+$ILC3 and B cell cocultures (**Fig 3, C**).

Interestingly, the IL-10-producing B cells in CD40L$^+$ILC3 and B cell cocultures were IL-6$^+$IL-10$^+$ on day 6, probably due to the initial CpG stimulation, however became IL-6$^-$IL-10$^+$ on day 12 (**Fig 5, C**). CD40L$^+$ILC3s were also IL-6$^+$ in 85.2±3.2% on day 6 and became IL-6$^-$ in 97.2±1.8% on day 12, however they did not produce significant amount of IL-10 at any time point.

Further characterization of the IL-10$^+$B cells demonstrated that on day 12 up to 45% of these cells showed a CD19$^+$IgD$^+$IgM$^+$CD24^{high}CD38^{high} itB cell phenotype. This was observable only in CD40L$^+$ILC3 cocultures and not in other control conditions (**Fig 5, D**).

Considering that B cells can contact both the abundant T cells and the relatively rare ILC3s in the tissues, we aimed to examine the difference between these two interactions in order to define the specific function of CD40L$^+$ILC3s. T cells were much weaker in the support of long term survival of itB cells compared to CD40L$^+$ILC3s, as on day 12 a lower relative abundance of itB cells was observed both within all B cells and within IL-10$^+$B cells in T cell and B cell cocultures compared to that of in CD40L$^+$ILC3 and B cell cocultures (**Fig 5, E**).

As an additional marker of regulatory phenotype, IL-10$^+$B cells expressed PD-L1 on their surface (**Fig 5, F**).

In order to prove that the developed IL-10$^+$B cells were *bona fide* regulatory B (B_{reg}) cells, B cells were isolated from CD40L$^+$ILC3 cocultures on day 12 and tested in a suppression assay. CD40L$^+$ILC3 coculture-derived B_{reg} cells were able to suppress tetanus toxoid-induced T cell proliferation in a dose-dependent manner. Their suppressive efficiency was comparable to that of regulatory T (T_{reg}) cells or rhIL-10 (10 ng/mL) and was dependent on IL-10 as it was inhibited by anti-IL-10-receptor blocking antibody (**Fig 5, G**).

Role of CD40L in ILC3-B cell interaction

B cell viability, IL-10^{+}B$_{reg}$ cell differentiation, both regulatory (IL-10, IL-1ra) and proinflammatory (IL-6) cytokine production and IgM secretion were strongly, and proliferative capacity was to a lesser extent dependent on ILC3-provided CD40L-mediated help. This was suggested by the observation that the absence of CD40L from the surface of ILC3s (in case of CD40L^{-}ILC3), or the inhibition of CD40-CD40L interaction by a neutralizing anti-CD40L antibody (**Fig 6, A-C**), as well as the physical prevention of cell-cell contact in transwell plate cocultures (**Fig 6, D-E**) resulted in a reduction of the B cell-supporting effects of ILC3s. Meanwhile, the viability of ILC3s was not affected by the physical separation of B cells in transwell cocultures (**Fig 6, D**). Moreover, the specific itB cell-inducing effects of CD40L^{+}ILC3s were still partially persisted even in the absence of cell-cell contact (in transwell cocultures; **Fig 6, F**).

B cell-activating factor (BAFF) and IL-15 are key players of bilateral ILC3-B cell interaction

CD40L^{+}ILC3s were able to produce BAFF in response to IFN-γ (**Fig 7, A**). BAFF is a key cytokine of B cell maturation [24] and survival [25]. Substantial amounts of IFN-γ are secreted spontaneously in tonsils [26], which can be further increased during immune responses against invading microorganisms (e.g. in bacterial infection) and thus, probably able to induce BAFF production in ILC3s *in vivo*. Moreover, B cells upregulated *IL15* mRNA expression upon interaction with CD40L^{+}ILC3s in cocultures (**Fig 7, B**). IL-15 production of B cells was induced only by CD40L^{+}ILC3s (not by L cells), and was inhibited by anti-BAFF-receptor (αBAFFr) blocking antibody (**Fig 7, C**). The growth and survival of ILC3s depended on IL-15, as they ceased to proliferate and died off within 6 days after withdrawal of this cytokine from the culture medium (see second column in **Fig 7, D**). To analyze the ILC3-supporting effects of B cells, we compared ILC3 survival in ILC3 alone cultures and B cell cocultures in the presence or absence of IL-15 supplementation. ILC3 survival was significantly higher in B cell cocultures compared to ILC3 alone cultures without IL-15 (**Fig 7, D**).

Blocking of BAFF-receptor did not influence the B cell viability, proliferation, IL-10-producing B cell differentiation, cytokine and IgM production in $CD40L^+$ILC3 and B cell cocultures (**Fig E7, A-E**). However, the itB cell-inducing effects of $CD40L^+$ILC3s were mediated – at least in part – via BAFF–BAFF-receptor interaction, as the relative abundance of itB cells was reduced by αBAFFr in cocultures (**Fig 7, E**).

To further clarify the role of BAFF in IL-15 production, we stimulated tonsillar naïve B cells with BAFF or CpG alone, or both together. BAFF and CpG stimulation induced *IL15* mRNA expression (**Fig 7, F**) and IL-15 production (**Fig 7, G**) in tonsil-derived naïve B cells isolated from non-allergic patients, but was not able to induce IL-15 in B cells of allergic patients.

ILC3s and IL-10^+B_{reg} cells colocalize in palatine tonsils *in vivo*

In order to demonstrate that the above-detailed peculiar interaction of ILC3s and B cells is operational *in vivo*, ILC3s ($ROR\gamma t^+CD3^-$) and B_{reg} cells ($CD20^+IL\text{-}10^+$) were visualized with immunofluorescence histology. These cells were in close contact with each other (**Fig 8, A**), were found in niches of regulatory cells that also harbor numerous $CD3^+IL10^+T_{reg}$ cells, and localized in the interfollicular area of palatine tonsils (**Fig E8, A**).

The relative abundance of ILC3s is reduced in allergic diseases

The relative frequency of ILC3 cell was lower in TMC lymphocytes isolated from palatine tonsil tissue of allergic compared to non-allergic patients (**Fig 8, B**). Both ILC3s and itB_{reg} cells were less abundant in the peripheral blood of patients with allergic asthma compared to healthy controls (**Fig 8, C** and **E8, B**); but the T_{reg} cells were equal in the two groups (**Fig E8, C**). The percentages of ILC3s positively correlated with itB_{reg} cells (**Fig 8, D**); while T_{reg} cell did not correlate with either ILC3s or itB_{reg} cells (**Fig E8, D and E**).

DISCUSSION

The present study provides evidence for the first time that activated, CD40L-expressing type 3 innate lymphoid cells ($CD40L^+$ILC3s) has a dedicated role in the induction of the immature transitional regulatory B (itB_{reg}) cells.

Human circulating $Lin^-CD4^-CD56^-$IL-$7R\alpha^+CD161^+$c-Kit^+ILC3s were able to differentiate into the recently identified[18], activated form of ILC3s, the $CD40L^+$ILC3, in response to IL-15. We used IL-15 to expand low numbers of ILC3s isolated either from peripheral blood or from palatine tonsil tissue samples, established $CD40L^+$ILC3 cell lines and demonstrated their functional properties. Tonsillar epithelial cells and mDCs may contribute to the supporting microenvironment of the $CD40L^+$ILC3s in the tissue via their IL-15 production. B cells can also secrete IL-15[27], and we demonstrated that BAFF, together with CpG stimulation induced IL-15 production in naïve B cells. Naïve B cells also upregulated IL-15 expression upon interaction with ILC3s, and the $CD40L^+$ILC3-induced IL-15 production was mediated by BAFF in a BAFF-receptor-dependent manner. Taken together, several lines of evidence indicate that $CD40L^+$ILC3s and B cells are in a mutually beneficial relationship, and B cells contribute to the ILC3-supporting microenvironment in the tissues. The high expression level of NKp44 on tonsillar ILC3s also suggests that there is an IL-15-rich microenvironment in tonsils, as NKp44 is upregulated by IL-15 in blood-derived ILC3s.

Without appropriate stimulation, B cell survival is very limited. However, our data clearly demonstrated that $CD40L^+$ILC3s strongly support naïve B cell survival and proliferation *in vitro*. The anatomical localization of ILC3s in human palatine tonsils enables them to encounter and contact B cells *in vivo*. The expression of the CD40L on the surface of ILC3s makes the interaction with B cells almost self-evident, because of the well-established, essential role of CD40-CD40L interaction in B cell activation, differentiation and survival[22, 28]. Moreover, both ILC3s and B cells express TLR9, and we demonstrated that the release of sCD40L, and thus the B cell-fostering capacity of the $CD40L^+$ILC3s, were increased upon stimulation with CpG. Besides CD40L expression, ILC3s are also able to produce BAFF[29],

another B cell stimulating factor[24]. Consequently, both spatial and contextual factors suggest that ILC3-B cell interaction takes place in tonsils, *in vivo*.

CD40L$^+$ILC3-mediated B cell help was specifically focused on immature transitional B cells. Moreover, here we reported that CD40L$^+$ILC3s have an extraordinary capacity to induce the development of IL-10-secreting, PD-L1-expressing, functional B_{reg} cells. The comparison of the B cell-supporting effects of ILC3s and T cells revealed that the specific role of CD40L$^+$ILC3s is particularly the induction of B_{reg} cells with immature transitional phenotype (itB_{reg}), and not only the induction B_{reg} cells in general. The CD19$^+$CD27$^-$ IgD$^+$IgM$^+$CD24^{high}CD38^{high}CD1d^{high}itB_{reg} cells[23] have a remarkable immunoregulatory capacity[15, 30-33], and are deficient and/or functionally impaired in autoimmune diseases (e.g. systemic lupus erythematosus[15], rheumatoid arthritis[32]). The expression of PD-L1, an inhibitory costimulatory molecule, may also contribute to the immunoregulatory function of B_{reg} cells[34-35].

Increasing evidence suggest[4] that ILC3s play key role in mucosal homeostasis and immunoregulation via IL-22 production[5, 8, 11-12], promotion of natural IgM secretion[18], limitation of immune responses against commensal bacteria[13], inhibition of Th17-mediated intestinal inflammation[36] and restoration of lymphoid tissue integrity after destructive infection[7]; consequently, the demonstrated ability of CD40L$^+$ILC3s to promote itB_{reg} cell differentiation fits well to the regulatory image[4] of the ILC3s.

B cells are known to produce IL-6 in response to innate stimulation with CpG, and the cytokine secretion is further increased in the presence of CD40L[37]. These stimuli also induce the secretion of the inhibitory cytokines (IL-10 and IL-1ra), however, typically they do not reach to high levels *in vitro*. Here we demonstrated that CD40L$^+$ILCs were potent inducers of cytokine-production by B cells. The seemingly contradictory activation state of the B cells (i.e. parallel production of IL-6 and IL-10) is a matter of a long-standing debate. A recent study suggested an explanation for this: IL-6 could be essential for the IL-10-producing B cell development[38]. Although the exact cellular sources of IL-6 have not been specified in that study, it has been shown that massive IL-6 production from mesenteric lymph node

lymphocytes and splenocytes, most probably including B cells and ILC3s, is required for normal B_{reg} cell development. In our $CD40L^+$ILC3 and B cell cocultures indeed both cell types were producing IL-6 in the early phase, on day 6 after activation with CpG, and this may facilitate differentiation of IL-10^+IL-6^- B_{reg} cells detected on day 12.

We showed that CD40-CD40L interaction plays a pivotal role in ILC3-B cell communication, as it was crucial for $CD40L^+$ILC3-induced B_{reg} cell development, as well as for cytokine and IgM production. ILC3-derived BAFF may also participate in itB_{reg} cell induction in human tonsils, as it is an important cytokine of the ILC3-B cell interplay. BAFF participates in T cell-independent help provided by DCs, macrophages, neutrophils and ILC3s to splenic marginal zone B cells and plasma cells[18], and it is known to induce IL-10-producing B_{reg} cells in mice[39]. $CD40L^+$ILC3s could produce BAFF, however we could not detect a proliferation-inducing ligand (APRIL) in these cells. We observed that $CD40L^+$ILC3s exerted an itB cell-inducing effect even in the absence of cell-cell contact (in transwell cocultures), consequently this can be partially mediated by soluble factor(s) including BAFF. BAFF signaling via BAFFr (TNFRSF13C) has a key role in B cell maturation, as transitional, follicular and marginal zone B cells numbers are strongly reduced in BAFFr-deficient mice[40]. We found that itB cell-inducing effect of ILC3s was also BAFF-dependent, as it was reduced by neutralization of BAFF-receptor.

Tonsils have been identified as important mucosal sites of immune tolerance[41], where the generation of functional allergen-specific T_{reg} cells occurs. We demonstrated that indeed RORγt^+CD3^- ILC3s and $CD20^+$IL-10^+B_{reg} cells colocalized in the palatine tonsils *in vivo*, they contacted each other, and were in the same regions as $CD3^+$IL-10^+T_{reg} cells. The data suggest that there are regulatory niches in tonsils where T_{reg} and B_{reg} cells develop next to each other. $CD40L^+$ILC3s may be involved in the maintenance of the immune tolerance in tonsils by the induction of functional itB_{reg} cells. These cells can contribute to the suppression of T cell responses both through cell-cell contact via PD-L1, and via secreted IL-10. These mechanisms may also play a role in immune tolerance-induction during successful sublingual immunotherapy[42-43].

The absolute numbers of T_{reg} cells and the expression level of Foxp3 in these cells are dependent on IL-10 production by B cells. The modulation of the T_{reg} cell frequencies *in vivo* is exclusively restricted to transitional 2 marginal zone precursor B_{reg} cells in mice[44]. In addition, human itB_{reg} cells are able to induce T_{reg} cells *in vitro*[45]. Of note, worm infection-induced $CD1d^{high}$ IL-10-producing B_{reg} cells can prevent and reverse airway inflammation in allergized mice by inducing the recruitment of T_{reg} cells to the lung[46]. T_{reg} cell percentages were not lower in allergic asthmatics and did not correlate with either ILC3s or itB_{reg} cells, suggesting that the peripheral blood T_{reg} cell levels may not mirror the immunoregulatory status, and these cells can be influenced by multiple factors.

Adoptive transfer of itB_{reg} cells can ameliorate allergic airway inflammation and hyper-responsiveness in mouse model of allergic asthma in an IL-10-dependent manner[47]. The relative proportion of various B_{reg} cell subsets within B cells was found to be reduced in allergic diseases (allergic rhinitis[48]; allergic asthma[49]), and the frequency of IL-10-producing, antigen-specific B cells increased after allergen-specific immunotherapy[35].

We demonstrated that ILC3s comprised a significantly smaller fraction of tonsillar lymphocytes in allergic compared to non-allergic patients. The frequency of ILC3s, expressed as percentage of all $CD45^+$ cells, has been reported to be unaltered in mild asthmatics (GINA step 1) with confounding allergic rhinoconjunctivitis compared to non-allergic controls[50]. However, we found significantly reduced circulating ILC3 numbers within all lymphocytes in highly selected, moderate-to-severe allergic asthmatic patients (GINA step 3 to 4) compared to healthy controls. There was a significant positive correlation between peripheral blood ILC3 and itB_{reg} cell percentages, and the lower ILC3 levels in allergic asthmatics were accompanied with lower itB_{reg} cell counts.

It was suggested by mouse models that IL-15 may have a protective role in allergic diseases[51-52]. We showed that the CpG- and BAFF-induced IL-15 production is deficient in tonsillar naïve B cells of allergic patients. This may represent a mechanism that contributes to the reduction of the size of circulating ILC3 pool.

Collectively, our experimental results indicate a strong itB_{reg} cell-inducing capacity of the activated ILC3s, therefore the reduced ILC3 levels may contribute to the insufficient B_{reg} cell-mediated immune tolerance in various allergic diseases including allergic asthma.

In conclusion, we have described here a novel, innate immunoregulatory function of $CD40L^+$ILC3s, an activated form of the type 3 innate lymphoid cells. $CD40L^+$ILC3s provide extrafollicular, T cell-independent B cell help in palatine tonsils and induce immature transitional B_{reg} cell development. This mechanism may contribute to the maintenance of immune tolerance to innocuous antigens and become insufficient in allergy. Further investigation is required to explore the possibility of the therapeutic interventions targeting ILC3 - B cell interaction in allergic diseases.

ACKNOWLEDGMENTS

Z.I.K. is the recipient of a European Respiratory Society Fellowship (LTRF55-2010). Funding: This work was supported by Swiss National Science Foundation grants 310030-156823, 320030–140772 and Christine Kühne-Center for Allergy Research and Education (CK-CARE), Davos, Switzerland.

COMPETING INTERESTS

The authors declare that they have no competing interests.

FIGURE LEGENDS

FIG 1. Expansion and differentiation of ILC3s

(**A**) Peripheral blood ILC3s were sorted according to the gating strategy shown in **FIG E1A**, expanded with IL-15 for 20 days and analyzed by flow cytometry. $CD94^{+}CD40L^{-}c\text{-}Kit^{low}$cNK cells, $CD94^{-}CD40L^{-}c\text{-}Kit^{high}$ILC3s (referred to as $CD40L^{-}$ILC3s) and $CD94^{-}CD40L^{+}c\text{-}Kit^{high}$ILC3s (referred to as $CD40L^{+}$ILC3s) are defined here. These cell populations were sorted for *in vitro* experiments. Quadrant statistics in table represents fourteen independent experiments.

(**B**) Tonsillar ILC3s were sorted according to the gating strategy shown in **FIG E1B**, expanded with IL-15 for 20 days and analyzed by flow cytometry. Tonsillar ILC3s differentiate mainly into $CD40L^{-}$ILC3s, and $CD40L^{+}$ILC3s. These cell populations were sorted for *in vitro* experiments. Quadrant statistics in table represents five independent experiments.

(**C**) Analysis of *IL15* mRNA in isolated tonsillar cell populations (*: $p<0.05$ vs Total TMC, $CD3^{+}$, $CD19^{+}$, and pDC; n=5; except pDC, mDC and Tonsillar Epithel n=3).

(**D**) NK cell receptor NKp44 expression in circulating ILC3s at isolation, after culture (IL-15, 20 days) and tonsillar ILC3 at isolation, analyzed by flow cytometry (*: $p<0.01$ vs blood ILC3 at isolation; n=3; except Blood ILC3+IL-15 n=4).

(**E**) *RORC* mRNA expression in blood-derived ILC3 subsets defined in **A.** (*: $p<0.05$ vs PBMC and cNK; n=4; except $CD40L^{+}$ILC3 n=5).

(**F**) Intranuclear RORγt protein levels in blood ILC3-derived cell subsets defined in **A**, analyzed by flow cytometry. (*: $p<0.01$ vs all other groups; #: $p<0.05$ vs ISO and cNK; n=3).

(**G**) IL-22 secretion of blood ILC3-derived cell subsets (defined in **A**) in response to IL-23 (*: $p<0.05$ vs $CD40L^{-}$ILC3 and cNK; #: $p<0.05$ vs cNK; n=4).

(**H**) *CD40LG* mRNA expression in tonsillar cell subpopulations sorted from fresh tissue samples (*: $p<0.01$ vs B cells; n=3).

(**I**) CD40L protein expression on tonsillar ILC3s cultured *ex vivo* for 36 hours with IL-15, analyzed by flow cytometry. The number indicates percent $CD40L^+$ cells. One representative experiment is shown out of two with similar results.

FIG 2. $CD40L^+$ILC3s support B cell survival, proliferation and IgM production

(**A**) (**B**) and (**C**) Blood-derived $CD40L^+$ILC3s and naïve B cells were cocultured in the indicated ratios, in the presence of IL-15 and an initial CpG stimulation. Naïve B cells were sorted according to the gating strategy shown in **Fig E6**. B cell survival and proliferation were analyzed on day 12 by flow cytometry. A viability dye, e-450 was used to discriminate between living and dead cells. Proliferation rate of the B cells was assessed by analysis of CFSE dilution and calculation of the proliferative index (numbers indicate percent proliferating cells in parent gate; nd: non-dividing). Statistical analyses of the coculture experiments are shown on (**B**) and (**C**). Cocultures of naïve B+L cells, as well as $CD40L^-$ ILC3s and naïve B cells were used as controls. (*: $p<0.05$ vs 1:15, $CD40L^-$ILC3:B cell coculture, and B alone; #: $p<0.05$ vs B alone; †: $p<0.05$ vs all other groups; n=10-15).

(**D**) Immunoglobulin production was measured by multiplex bead assay in cell (co)culture supernatants (day 12; *: $p<0.05$ vs 1:15, $CD40L^-$ILC3:B cell coculture, B alone and B+L cells coculture; n=7-10).

FIG 3. Tonsil-derived $CD40L^+$ILC3s supported B cell survival, proliferation and induced IL-10-producing B cell differentiation

(**A**) and (**B**) Tonsil-derived $CD40L^+$ILC3s and tonsillar naïve B cells were cocultured in 1:1, 1:3 and 1:7 ratios in the presence of IL-15 and an initial CpG stimulation. B cell survival (**A**) and B cell proliferation (**B**) were analyzed on day 12 by flow cytometry. A viability dye, e-450 was used to discriminate between living and dead cells. Proliferation rate of the B cells was assessed by flow cytometric analysis of CFSE dilution in the dividing cells, and calculation of the proliferative index. Cocultures of tonsillar naïve B cells + L cells were used as controls. (*: $p<0.05$ vs 1:7 and B alone; #: $p<0.05$ vs B alone; †: $p<0.05$ vs all other groups; n=5).

(**C**) IL-10-producing B cells in tonsil-derived cocultures and B cell alone cultures on day 12, analyzed by flow cytometry. The plot is gated on all viable cells of a representative tonsil-derived $CD40L^+$ILC3 and B cell (1:3) coculture. $IL\text{-}10^+$B cell populations are shown as percent of all viable $CD19^+$ cells (#: $p<0.05$ vs B alone; n=3).

FIG 4. $CD40L^+$ILC3-mediated B cell help is specifically focused on immature transitional B cells

(**A**) $CD40L^+$ILC3 and B cell (1:3) coculture on day 12, analyzed by flow cytometry. The first plot is gated on all viable cells. Immature transitional B (itB) cells were defined as c-Kit^- $CD19^+CD27^-IgD^+IgM^+CD24^{high}CD38^{high}CD1d^{high}$. IgM single-positive cells were c-Kit^- $CD19^+CD27^-IgD^-IgM^+CD24^{low}CD38^{low}CD1d^{low}$ (representative of seven independent experiments).

(**B**) Proliferation rates of total B cells, itB cells and IgM single-positive B cells in a $CD40L^+$ILC3 and B cell (1:3) coculture on day 12, analyzed by flow cytometry. (*: $p<0.05$ vs B cells and IgM single-positive B cells; n=5).

(**C**) Flow cytometric comparison of itB cells (defined in **A**) between $CD40L^+$ILC3 and B cell cocultures, $CD40L^-$ILC3 and B cell cocultures, B+L cell cocultures and B cells alone cultures. All dotplots were gated on viable $CD19^+IgD^+IgM^+$ B cells on day 6. ItB cells are shown in the graph as percent of all viable $CD19^+$ B cells (#: $p<0.05$ vs other cultures; *: $p<0.01$ vs other cultures; n=5).

(**D**) ItB cells in freshly isolated TMC samples, analyzed by flow cytometry. First plot is gated on $CD19^+CD27^-$ B cells. One representative experiment is shown out of two with similar results.

Numbers in flow cytometric plots indicate percent cells in parent gate.

FIG 5. $CD40L^+$ILC3s induce the development of IL-10-secreting B regulatory cells

(**A**) Cytokine levels in cocultures and B cell alone cultures were measured by multiplex bead assay on day 6 (*: $p<0.05$ vs $CD40L^+$ILC3 alone, 1:7 and 1:15 $CD40L^+$ILC3:B cell cocultures,

567 $CD40L^-$ILC3:B cell coculture, B+L cells and B alone; #: p<0.05 vs $CD40L^+$ILC3 alone, 1:15
568 $CD40L^+$ILC3:B cell coculture and B alone; &: p<0.05 vs $CD40L^+$ILC3 alone, 1:15
569 $CD40L^+$ILC3:B cell coculture, B+L cells and B alone; †: p<0.05 vs all other cultures; n=10-
570 15).

571 (**B**) IL-10-producing B cells in cocultures and B cell alone cultures. The plot is gated on all
572 viable cells. IL-10^+B cells are shown as percent of all viable $CD19^+$ B cells (*: p<0.05 vs 1:7
573 and 1:15 $CD40L^+$ILC3:B cell cocultures, $CD40L^-$ILC3:B cell coculture, B+L cells and B alone;
574 #: p<0.05 vs $CD40L^-$ILC3:B cell coculture, B+L cells and B alone; †: p<0.05 vs $CD40L^-$
575 ILC3:B cell coculture and B alone; n/a: not available; n=8-13).

576 (**C**) Intracellular IL-6 and IL-10 content of B cells in 1:3 $CD40L^+$ILC3:B cell coculture. Plots
577 are gated on all viable B cells. One representative experiment is shown out of two with
578 similar results.

579 (**D**) Presence of itB cells in IL-10^+B cells. The first dotplot is gated on IL-10^+B cells developed
580 in a $CD40L^+$ILC3 and B cell coculture (day 6). The relative abundance of
581 $IgD^+IgM^+CD24^{high}CD38^{high}$ itB cells was compared between various cell cultures on day 6 and
582 12, and shown in the graph. (*: p<0.05 vs all other cultures; n=5).

583 (**E**) Comparison of the relative abundance of $IgD^+IgM^+CD24^{high}CD38^{high}$ itB cells between
584 $CD40L^+$ILC3 and B cell cocultures, and T cell and B cell cocultures. ItB cells are shown as
585 percent of all viable $CD19^+$ B cells, and also as percent of all viable $CD19^+$IL-10^+B cells (*:
586 p<0.05 vs CD40L+ILC3 and B cell coculture; day 12; n=2).

587 (**F**) Expression of regulatory cell marker PD-L1 on the surface of IL-10^+ and IL-10^- B cells in
588 $CD40L^+$ILC3 and B cell cocultures (*: p<0.05 vs IL-10^- B cells; day 12; n=2).

589 (**G**) Viable B cells were sorted from $CD40L^+$ILC3 cocultures on day 12, and cocultured with
590 CFSE-labeled PBMC (in 1:5; 1:10 and 1:20 ratio) in the presence of an anti-IL-10-receptor
591 blocking (αIL-10R) or isotype control (ISO) antibody. Tetanus toxoid (TT)-induced $CD4^+$ T
592 cell proliferation was analyzed. Freshly sorted autologous T_{reg} ($CD3^+CD4^+$IL-$7R\alpha^-CD25^+$) and
593 PBMC cocultures (in 1:10 and 1:20 ratio), and rhIL-10 (10 ng/mL) treated PBMC were used
594 as controls (*: p<0.05 vs PBMC; n=2).

(**B-G)** Data were analyzed by flow cytometry, numbers in plots indicate percent in parent gate.

FIG 6. Role of CD40L in the CD40L$^+$ILC3-B cell interaction

(**A**) We examined CD40L$^+$ILC3 and B cell, as well as CD40L$^-$ILC3 and B cell cocultures (both 1:3) treated with anti-CD40L neutralizing antibody (αCD40L) or isotype control antibody (ISO). B cell survival, proliferation and IL-10-producing B cell differentiation were analyzed (*: $p<0.05$ vs ISO-treated CD40L$^+$ILC3:B cell cocultures, ns: $p>0.05$ vs ISO-treated CD40L$^-$ ILC3:B cell cocultures; n=3).

(**B**) Cytokine levels were measured in cell culture supernatants by multiplex bead assay (*: $p<0.05$ vs ISO-treated CD40L$^+$ILC3:B cell cocultures; n=3).

(**C**) Immonoglobulin M (IgM) concentrations were measured in cell culture supernatants by multiplex bead assay (*: $p<0.05$ vs ISO-treated CD40L$^+$ILC3 and B cell cocultures; n=3).

(**D-F**) In order to examine the importance of cell-cell contact, CD40L$^+$ILC3s and B cells were cocultured in transwell plates.

(**D**) B cell and CD40L$^+$ILC3 viability was analyzed in normal coculture (Control) and in Transwell coculture(*: $p<0.05$ vs Transwell; n=2; e-780: viability dye).

(**E**) Intracellular IL-6 and IL-10 content of B cells in Control and Transwell CD40L$^+$ILC3s and B cell cocultures on day 6. Plots are gated on all viable CD19$^+$ B cells. (*: $p<0.05$ vs Transwell; n=2).

(**F**) ItB cells in Control and Transwell CD40L$^+$ILC3s:B cell cocultures on day 6. Dotplots are gated on viable CD19$^+$IgD$^+$IgM$^+$ B cells. The relative abundance of IgD$^+$IgM$^+$CD24^{high}CD38^{high} itB cells was compared between Control and Transwell cocultures (ns: $p>0.05$ vs Control; n=2).

(A) and (**B-G)** Data were analyzed by flow cytometry, numbers indicate percent cells in parent gate.

FIG 7. The role of BAFF and IL-15 in CD40L$^+$ILC3-B cell interaction

(**A**) BAFF expression of $CD40L^+$ILC3s in response to IFN-γ stimulation. One representative experiment is shown out of two with similar results.

(**B**) *IL15* mRNA expression in B cells in response to coculturing $CD40L^+$ILC3s or irradiated L cells (*: $p<0.05$ vs B cells alone and B+L cells; n=2).

(**C**) Intracellular IL-15 content of B cells in 1:3 $CD40L^+$ILC3:B cell coculture on day 12. Effects of BAFF-receptor blocking (αBAFFr) or isotype control (ISO) antibody on IL-15 expression. Histogram is gated on all viable B cells. Percentage of the $IL\text{-}15^+$ B cells was analyzed (*: $p<0.05$ vs ISO; n=2).

(**D**) Viability of $CD40L^+$ILC3 in B cell cocultures and alone with or without IL-15 on day 6 (*: $p<0.05$ vs $CD40L^+$ILC3 alone without IL-15; $CD40L^+$ILC3 alone n=3-4; $CD40L^+$ILC3 cocultures n=6-8).

(**E**) The relative abundance of $IgD^+IgM^+CD24^{high}CD38^{high}$ itB cells was compared between αBAFFr and ISO treated $CD40L^+$ILC3s and B cell cocultures on day 6. Dotplots are gated on viable $CD19^+IgD^+IgM^+$ B cells. (*: $p<0.05$ vs ISO; n=2).

(**F**) Naïve B cells were isolated from tonsil tissue, and stimulated with CpG and/or BAFF for 4 days. *IL15* mRNA expression were compared between samples of allergic and non-allergic patients (*: $p<0.05$ vs Non-allergic; n=4).

(**G**) Intracellular IL-15 content of tonsillar naïve B cells after 4 days of CpG and BAFF stimulation. Plots are gated on all viable B cells (*: $p<0.05$ vs Non-allergic; n=4).

(**A**), (**C**), (**D**), (**E**), and (**G**) Data were analyzed by flow cytometry, numbers indicate percent cells in parent gate.

FIG 8. Colocalization of ILC3s and IL-10^+B_{reg} cells in the regulatory cell niches of palatine tonsils; interrelation of ILC3s and itB_{reg} cells in allergy.

(**A**) Immunofluorescence histology of tonsils. $ROR\gamma t^+CD3^-$ ILC3s and $CD20^+IL\text{-}10^+B_{reg}$ cells are in close contact with each other *in vivo*. $CD3^+IL\text{-}10^+T_{reg}$ cells are also localized in the same region of the tissue. The localization of the ILC3s, B_{reg} cells and T_{reg} cells is demonstrated with a collection of pictures from different sections because the ILC3s are

relatively rare. Filled arrows: RORγt^{+}CD3^{-} ILC3s; open arrows: CD20^{+}IL-10^{+}B$_{reg}$ cells; asterisk: CD3^{+}IL-10^{+}T$_{reg}$ cells. Bright-field pictures (BF) are shown in the rightmost column. Representative isotype control stainings are shown in the lower row.

Representative images of three independent experiments. Scale bar is 20 μm.

(**B**) Percentage of ILC3s in tonsillar lymphocytes of allergic and non-allergic patients (ILC3s were gated according to the strategy shown in **Fig. E1B**; *: $p<0.05$ Allergic vs Non-allergic).

(**C**) Percentage of ILC3s in peripheral blood lymphocytes of allergic asthma patients and healthy controls (ILC3s were gated according to the strategy shown in **Fig. E1A**; *: $p<0.01$ Allergic asthma vs Healthy).

(**D**) Correlation between ILC3 and CD19^{+}IgD^{+}IgM^{+}CD24^{high}CD38^{high}CD1d^{high}PD-L1^{+} itB$_{reg}$ cell percentages in peripheral blood lymphocytes of allergic asthma patients (triangle) and healthy controls (circle).

REFERENCES

1. Mjosberg J, Spits H. Human Innate Lymphoid Cells. J Allergy Clin Immunol 2016; 138:1265-76.
2. Artis D, Spits H. The biology of innate lymphoid cells. Nature 2015; 517:293-301.
3. Zhang X. Regulatory functions of innate-like B cells. Cell Mol Immunol 2013; 10:113-21.
4. Klose CS, Artis D. Innate lymphoid cells as regulators of immunity, inflammation and tissue homeostasis. Nat Immunol 2016; 17:765-74.
5. Sawa S, Lochner M, Satoh-Takayama N, Dulauroy S, Berard M, Kleinschek M, et al. RORgammat+ innate lymphoid cells regulate intestinal homeostasis by integrating negative signals from the symbiotic microbiota. Nat Immunol 2011; 12:320-6.
6. Romera-Hernandez M, Aparicio-Domingo P, Cupedo T. Damage control: Rorgammat+ innate lymphoid cells in tissue regeneration. Curr Opin Immunol 2013; 25:156-60.
7. Scandella E, Bolinger B, Lattmann E, Miller S, Favre S, Littman DR, et al. Restoration of lymphoid organ integrity through the interaction of lymphoid tissue-inducer cells with stroma of the T cell zone. Nat Immunol 2008; 9:667-75.
8. Aparicio-Domingo P, Romera-Hernandez M, Karrich JJ, Cornelissen F, Papazian N, Lindenbergh-Kortleve DJ, et al. Type 3 innate lymphoid cells maintain intestinal epithelial stem cells after tissue damage. J Exp Med 2015; 212:1783-91.
9. Li Z, Hodgkinson T, Gothard EJ, Boroumand S, Lamb R, Cummins I, et al. Epidermal Notch1 recruits RORgamma(+) group 3 innate lymphoid cells to orchestrate normal skin repair. Nat Commun 2016; 7:11394.
10. Crellin NK, Trifari S, Kaplan CD, Cupedo T, Spits H. Human NKp44+IL-22+ cells and LTi-like cells constitute a stable RORC+ lineage distinct from conventional natural killer cells. J Exp Med 2010; 207:281-90.
11. Sanos SL, Vonarbourg C, Mortha A, Diefenbach A. Control of epithelial cell function by interleukin-22-producing RORgammat+ innate lymphoid cells. Immunology 2011; 132:453-65.
12. Guo X, Qiu J, Tu T, Yang X, Deng L, Anders RA, et al. Induction of innate lymphoid cell-derived interleukin-22 by the transcription factor STAT3 mediates protection against intestinal infection. Immunity 2014; 40:25-39.
13. Hepworth MR, Fung TC, Masur SH, Kelsen JR, McConnell FM, Dubrot J, et al. Immune tolerance. Group 3 innate lymphoid cells mediate intestinal selection of commensal bacteria-specific CD4(+) T cells. Science 2015; 348:1031-5.
14. Rosser EC, Mauri C. Regulatory B cells: origin, phenotype, and function. Immunity 2015; 42:607-12.
15. Blair PA, Norena LY, Flores-Borja F, Rawlings DJ, Isenberg DA, Ehrenstein MR, et al. CD19(+)CD24(hi)CD38(hi) B cells exhibit regulatory capacity in healthy individuals but are functionally impaired in systemic Lupus Erythematosus patients. Immunity 2010; 32:129-40.
16. Fukuoka A, Futatsugi-Yumikura S, Takahashi S, Kazama H, Iyoda T, Yoshimoto T, et al. Identification of a novel type 2 innate immunocyte with the ability to enhance IgE production. Int Immunol 2013; 25:373-82.

17. Tsuji M, Suzuki K, Kitamura H, Maruya M, Kinoshita K, Ivanov, II, et al. Requirement for lymphoid tissue-inducer cells in isolated follicle formation and T cell-independent immunoglobulin A generation in the gut. Immunity 2008; 29:261-71.

18. Magri G, Miyajima M, Bascones S, Mortha A, Puga I, Cassis L, et al. Innate lymphoid cells integrate stromal and immunological signals to enhance antibody production by splenic marginal zone B cells. Nat Immunol 2014; 15:354-64.

19. Liu CC, Perussia B, Young JD. The emerging role of IL-15 in NK-cell development. Immunol Today 2000; 21:113-6.

20. Gil-Cruz C, Perez-Shibayama C, Onder L, Chai Q, Cupovic J, Cheng HW, et al. Fibroblastic reticular cells regulate intestinal inflammation via IL-15-mediated control of group 1 ILCs. Nat Immunol 2016; 17:1388-96.

21. Huggins J, Pellegrin T, Felgar RE, Wei C, Brown M, Zheng B, et al. CpG DNA activation and plasma-cell differentiation of CD27- naive human B cells. Blood 2007; 109:1611-9.

22. Pietravalle F, Lecoanet-Henchoz S, Blasey H, Aubry JP, Elson G, Edgerton MD, et al. Human native soluble CD40L is a biologically active trimer, processed inside microsomes. J Biol Chem 1996; 271:5965-7.

23. Sims GP, Ettinger R, Shirota Y, Yarboro CH, Illei GG, Lipsky PE. Identification and characterization of circulating human transitional B cells. Blood 2005; 105:4390-8.

24. Schneider P, Takatsuka H, Wilson A, Mackay F, Tardivel A, Lens S, et al. Maturation of marginal zone and follicular B cells requires B cell activating factor of the tumor necrosis factor family and is independent of B cell maturation antigen. J Exp Med 2001; 194:1691-7.

25. Mackay F, Schneider P. Cracking the BAFF code. Nat Rev Immunol 2009; 9:491-502.

26. Quiding M, Granstrom G, Nordstrom I, Ferrua B, Holmgren J, Czerkinsky C. High frequency of spontaneous interferon-gamma-producing cells in human tonsils: role of local accessory cells and soluble factors. Clin Exp Immunol 1993; 91:157-63.

27. Schneider R, Mohebiany AN, Ifergan I, Beauseigle D, Duquette P, Prat A, et al. B cell-derived IL-15 enhances CD8 T cell cytotoxicity and is increased in multiple sclerosis patients. J Immunol 2011; 187:4119-28.

28. Banchereau J, Bazan F, Blanchard D, Briere F, Galizzi JP, van Kooten C, et al. The CD40 antigen and its ligand. Annu Rev Immunol 1994; 12:881-922.

29. Cella M, Otero K, Colonna M. Expansion of human NK-22 cells with IL-7, IL-2, and IL-1beta reveals intrinsic functional plasticity. Proc Natl Acad Sci U S A 2010; 107:10961-6.

30. Simon Q, Pers JO, Cornec D, Le Pottier L, Mageed RA, Hillion S. In-depth characterization of CD24(high)CD38(high) transitional human B cells reveals different regulatory profiles. J Allergy Clin Immunol 2016; 137:1577-84 e10.

31. Das A, Ellis G, Pallant C, Lopes AR, Khanna P, Peppa D, et al. IL-10-producing regulatory B cells in the pathogenesis of chronic hepatitis B virus infection. J Immunol 2012; 189:3925-35.

32. Flores-Borja F, Bosma A, Ng D, Reddy V, Ehrenstein MR, Isenberg DA, et al. CD19+CD24hiCD38hi B cells maintain regulatory T cells while limiting TH1 and TH17 differentiation. Sci Transl Med 2013; 5:173ra23.

33. Newell KA, Asare A, Kirk AD, Gisler TD, Bourcier K, Suthanthiran M, et al. Identification of a B cell signature associated with renal transplant tolerance in humans. J Clin Invest 2010; 120:1836-47.

34. Khan AR, Hams E, Floudas A, Sparwasser T, Weaver CT, Fallon PG. PD-L1hi B cells are critical regulators of humoral immunity. Nat Commun 2015; 6:5997.

35. van de Veen W, Stanic B, Yaman G, Wawrzyniak M, Sollner S, Akdis DG, et al. IgG4 production is confined to human IL-10-producing regulatory B cells that suppress antigen-specific immune responses. J Allergy Clin Immunol 2013; 131:1204-12.

36. Qiu J, Guo X, Chen ZM, He L, Sonnenberg GF, Artis D, et al. Group 3 innate lymphoid cells inhibit T-cell-mediated intestinal inflammation through aryl hydrocarbon receptor signaling and regulation of microflora. Immunity 2013; 39:386-99.

37. Vollmer J, Jurk M, Samulowitz U, Lipford G, Forsbach A, Wullner M, et al. CpG oligodeoxynucleotides stimulate IFN-gamma-inducible protein-10 production in human B cells. J Endotoxin Res 2004; 10:431-8.

38. Rosser EC, Oleinika K, Tonon S, Doyle R, Bosma A, Carter NA, et al. Regulatory B cells are induced by gut microbiota-driven interleukin-1beta and interleukin-6 production. Nat Med 2014; 20:1334-9.

39. Yang M, Sun L, Wang S, Ko KH, Xu H, Zheng BJ, et al. Novel function of B cell-activating factor in the induction of IL-10-producing regulatory B cells. J Immunol 2010; 184:3321-5.

40. Sasaki Y, Casola S, Kutok JL, Rajewsky K, Schmidt-Supprian M. TNF family member B cell-activating factor (BAFF) receptor-dependent and -independent roles for BAFF in B cell physiology. J Immunol 2004; 173:2245-52.

41. Palomares O, Ruckert B, Jartti T, Kucuksezer UC, Puhakka T, Gomez E, et al. Induction and maintenance of allergen-specific FOXP3+ Treg cells in human tonsils as potential first-line organs of oral tolerance. J Allergy Clin Immunol 2012; 129:510-20, 20 e1-9.

42. Palomares O, Martin-Fontecha M, Lauener R, Traidl-Hoffmann C, Cavkaytar O, Akdis M, et al. Regulatory T cells and immune regulation of allergic diseases: roles of IL-10 and TGF-beta. Genes Immun 2014; 15:511-20.

43. Moingeon P. Update on immune mechanisms associated with sublingual immunotherapy: practical implications for the clinician. J Allergy Clin Immunol Pract 2013; 1:228-41.

44. Carter NA, Vasconcellos R, Rosser EC, Tulone C, Munoz-Suano A, Kamanaka M, et al. Mice lacking endogenous IL-10-producing regulatory B cells develop exacerbated disease and present with an increased frequency of Th1/Th17 but a decrease in regulatory T cells. J Immunol 2011; 186:5569-79.

45. Lemoine S, Morva A, Youinou P, Jamin C. Human T cells induce their own regulation through activation of B cells. J Autoimmun 2011; 36:228-38.

46. Amu S, Saunders SP, Kronenberg M, Mangan NE, Atzberger A, Fallon PG. Regulatory B cells prevent and reverse allergic airway inflammation via FoxP3-positive T regulatory cells in a murine model. J Allergy Clin Immunol 2010; 125:1114-24 e8.

47. Braza F, Chesne J, Durand M, Dirou S, Brosseau C, Mahay G, et al. A regulatory CD9(+) B-cell subset inhibits HDM-induced allergic airway inflammation. Allergy 2015; 70:1421-31.

48. Kim AS, Doherty TA, Karta MR, Das S, Baum R, Rosenthal P, et al. Regulatory B cells and T follicular helper cells are reduced in allergic rhinitis. J Allergy Clin Immunol 2016; 138:1192-5 e5.

49. Kamekura R, Shigehara K, Miyajima S, Jitsukawa S, Kawata K, Yamashita K, et al. Alteration of circulating type 2 follicular helper T cells and regulatory B cells underlies

the comorbid association of allergic rhinitis with bronchial asthma. Clin Immunol 2015; 158:204-11.

50. Lombardi V, Beuraud C, Neukirch C, Moussu H, Morizur L, Horiot S, et al. Circulating innate lymphoid cells are differentially regulated in allergic and nonallergic subjects. J Allergy Clin Immunol 2016; 138:305-8.

51. Aoi N, Masuda T, Murakami D, Yajima T, Mizubuchi H, Yamada H, et al. IL-15 prevents allergic rhinitis through reactivation of antigen-specific CD8+ cells. J Allergy Clin Immunol 2006; 117:1359-66.

52. Ishimitsu R, Nishimura H, Yajima T, Watase T, Kawauchi H, Yoshikai Y. Overexpression of IL-15 in vivo enhances Tc1 response, which inhibits allergic inflammation in a murine model of asthma. J Immunol 2001; 166:1991-2001.

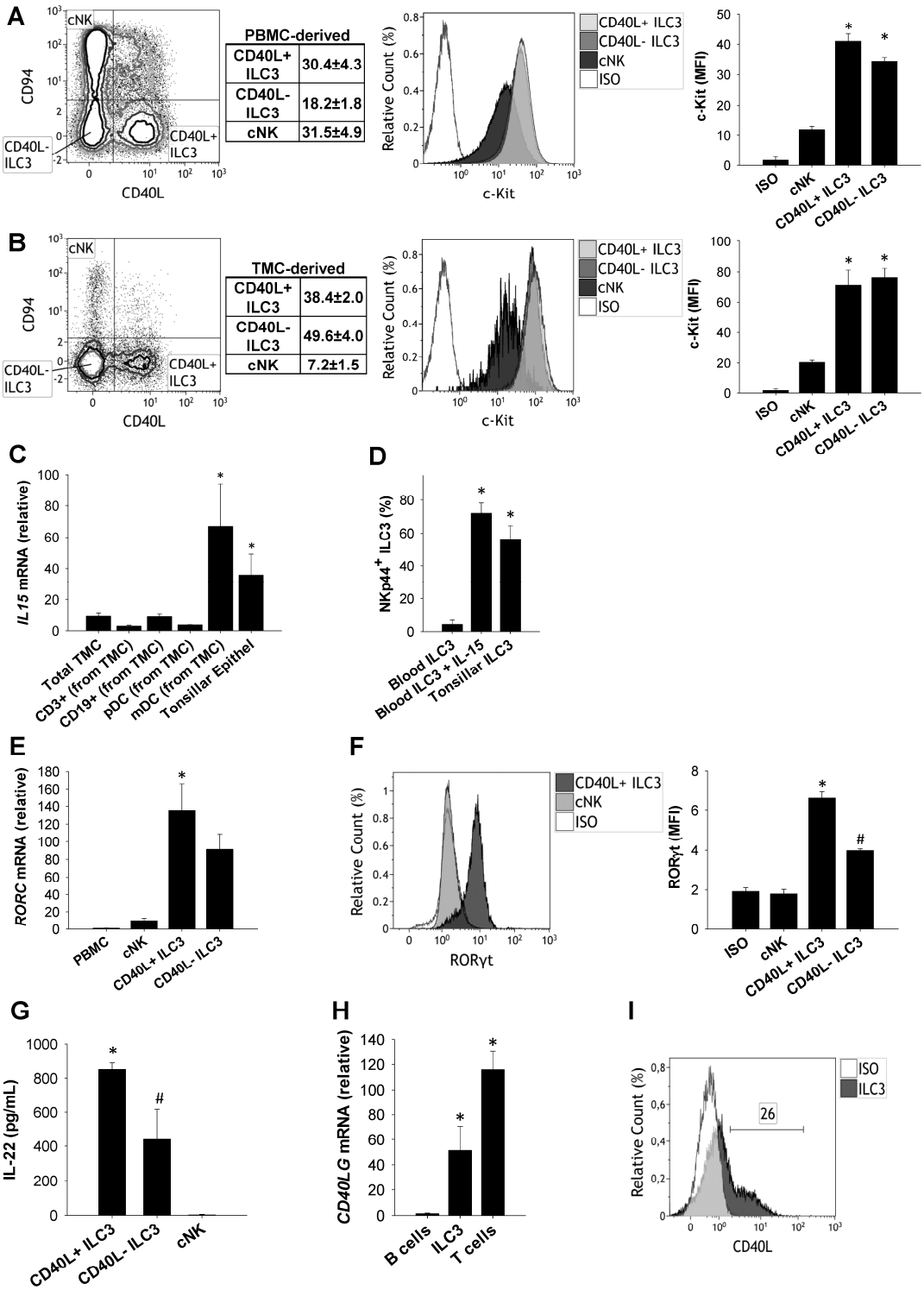

Figure 1 Komlósi ZI et al.

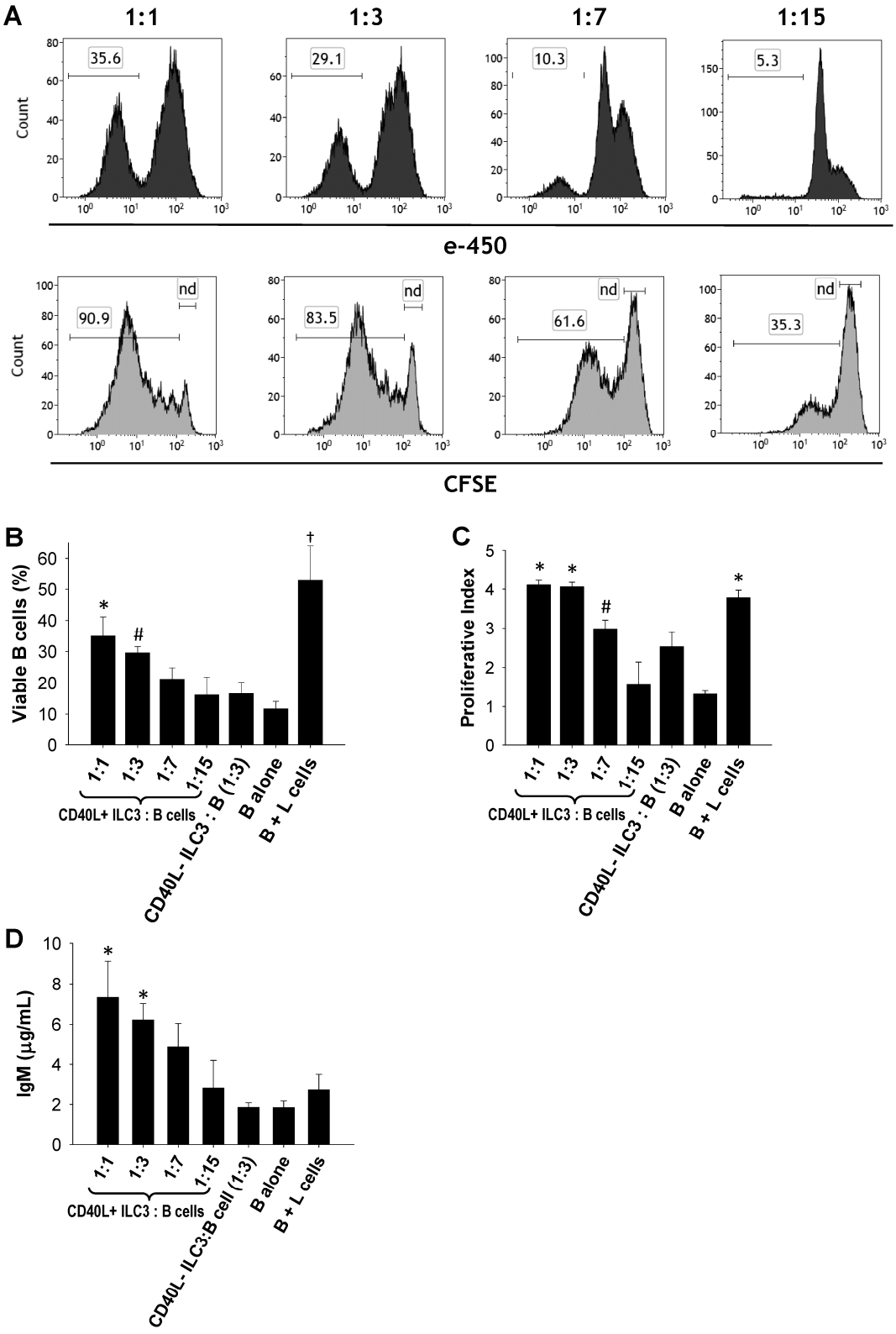

Figure 2 Komlósi ZI et al.

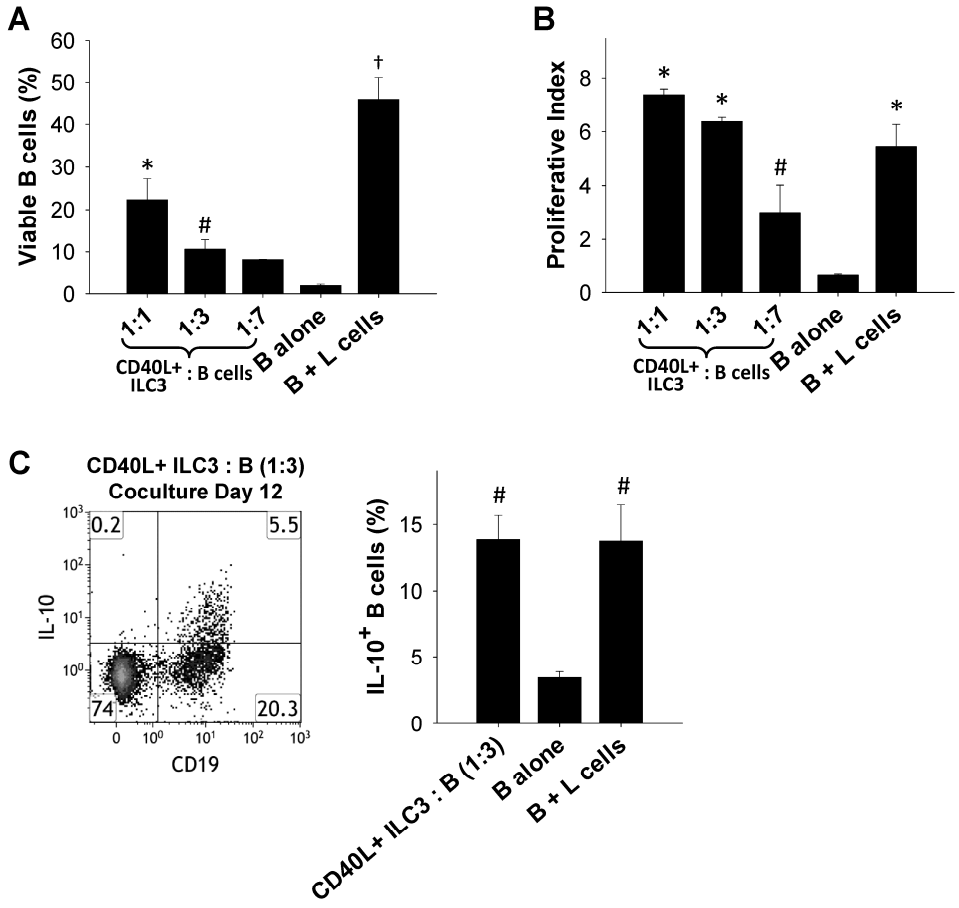

Figure 3 Komlósi ZI et al.

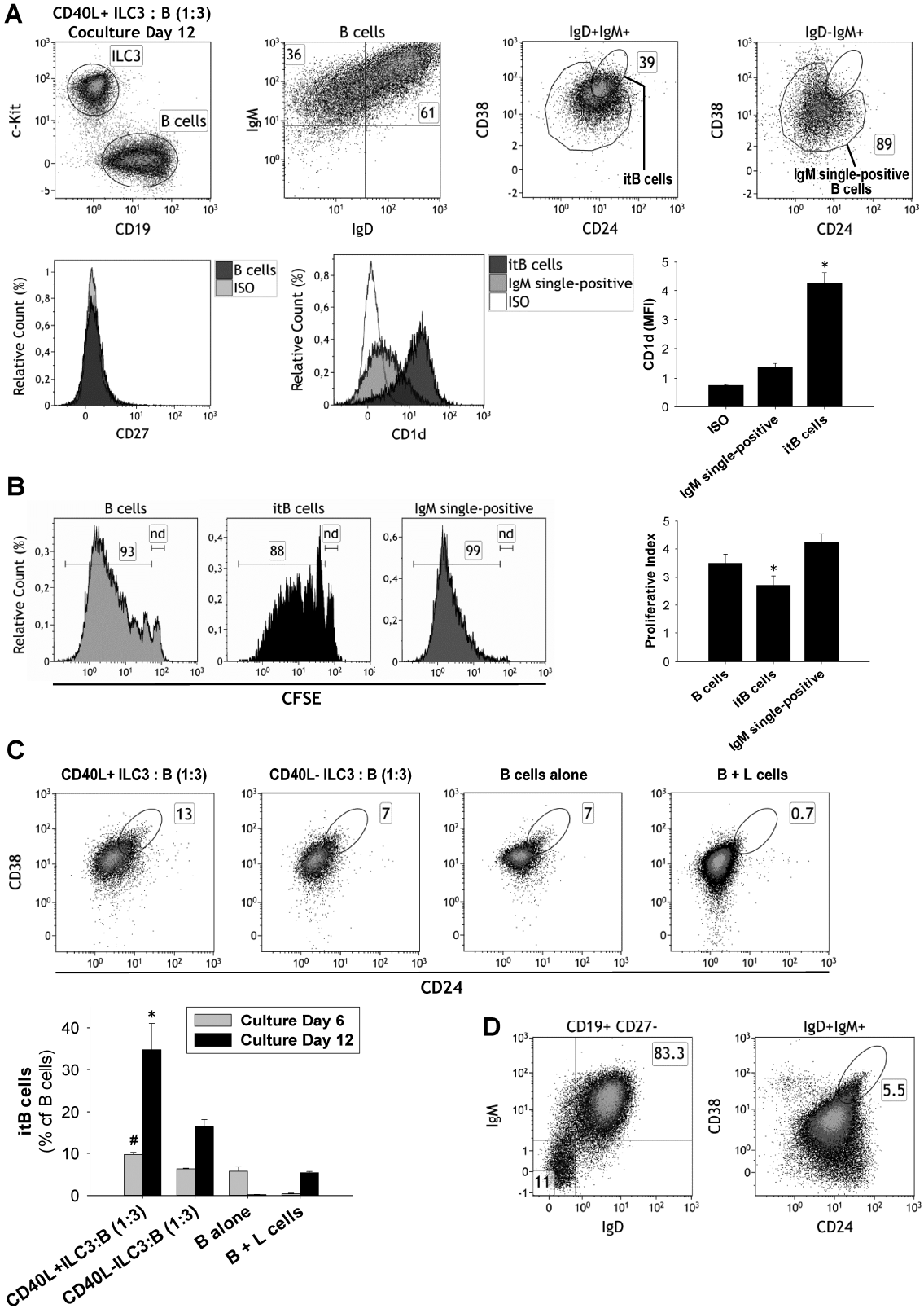

Figure 4 Komlósi ZI et al.

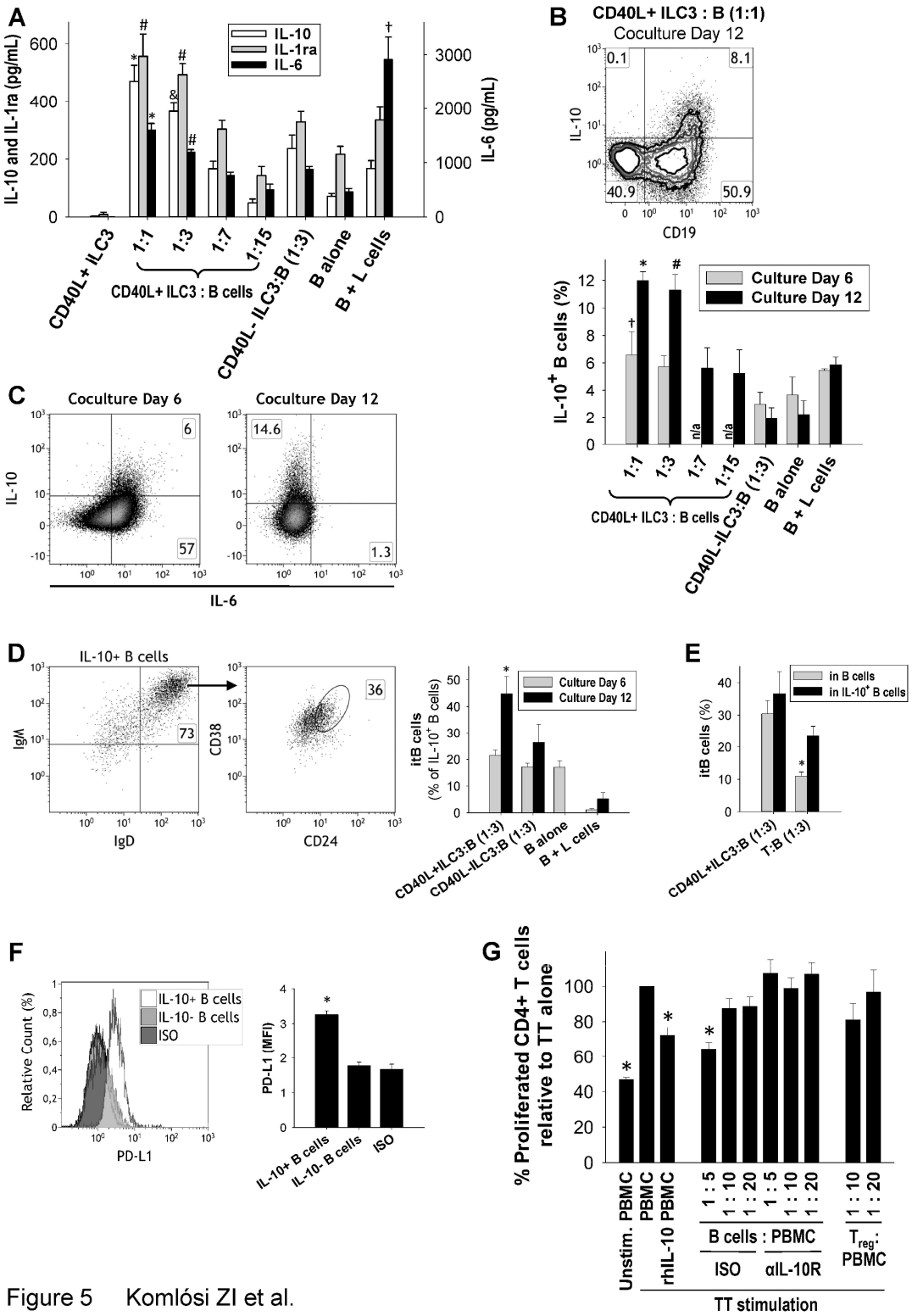

Figure 5 Komlósi ZI et al.

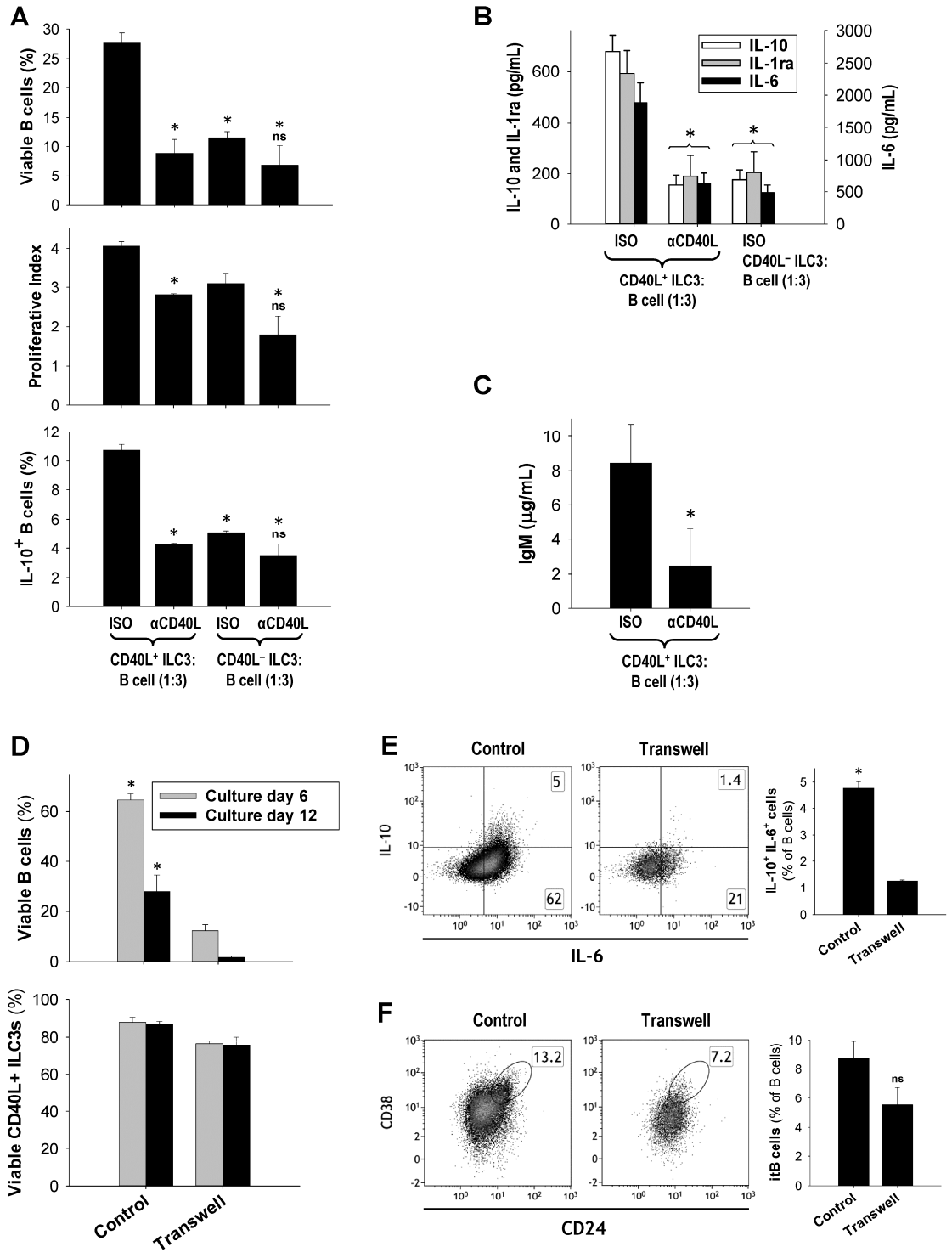

Figure 6 Komlósi ZI et al.

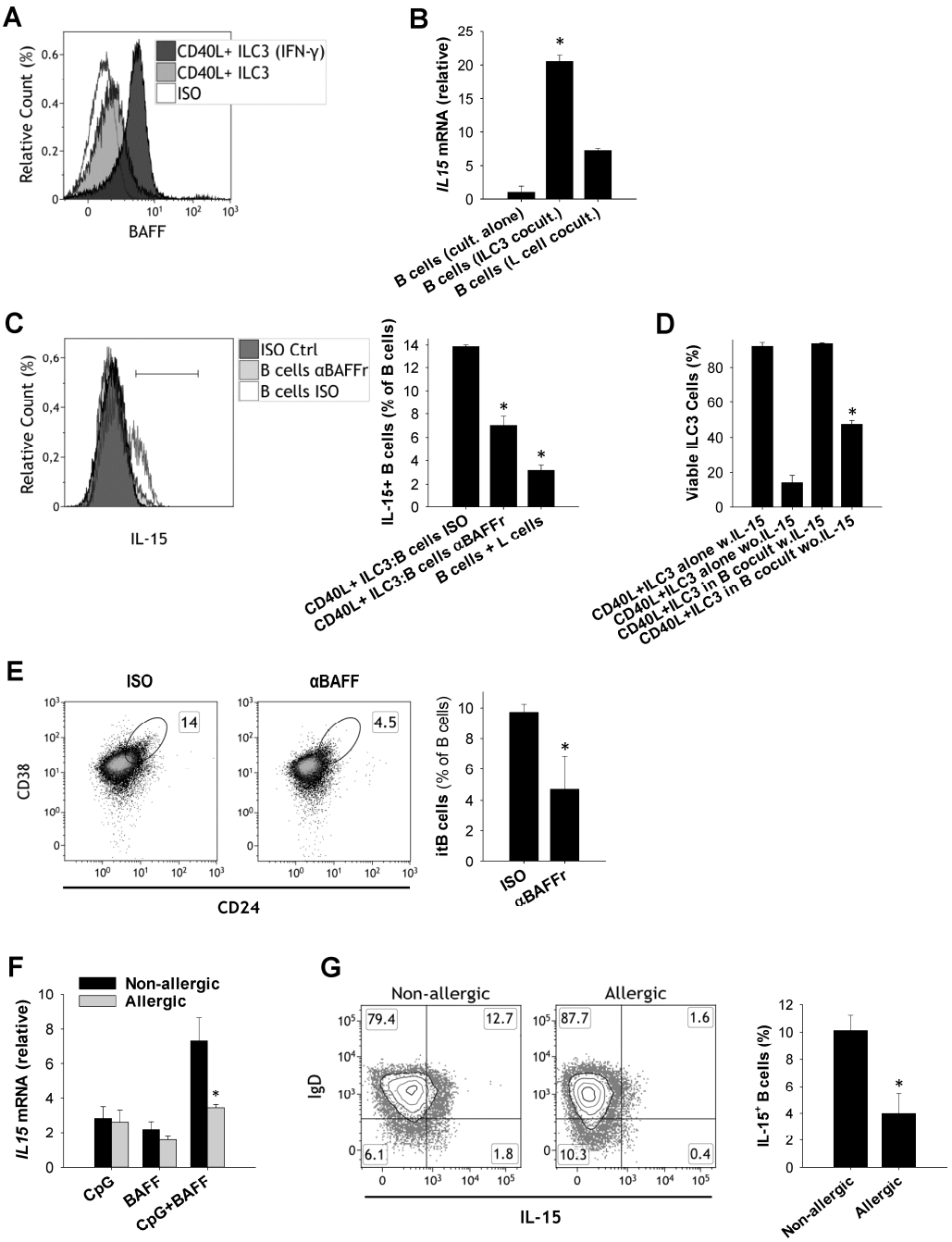

Figure 7 Komlósi ZI et al.

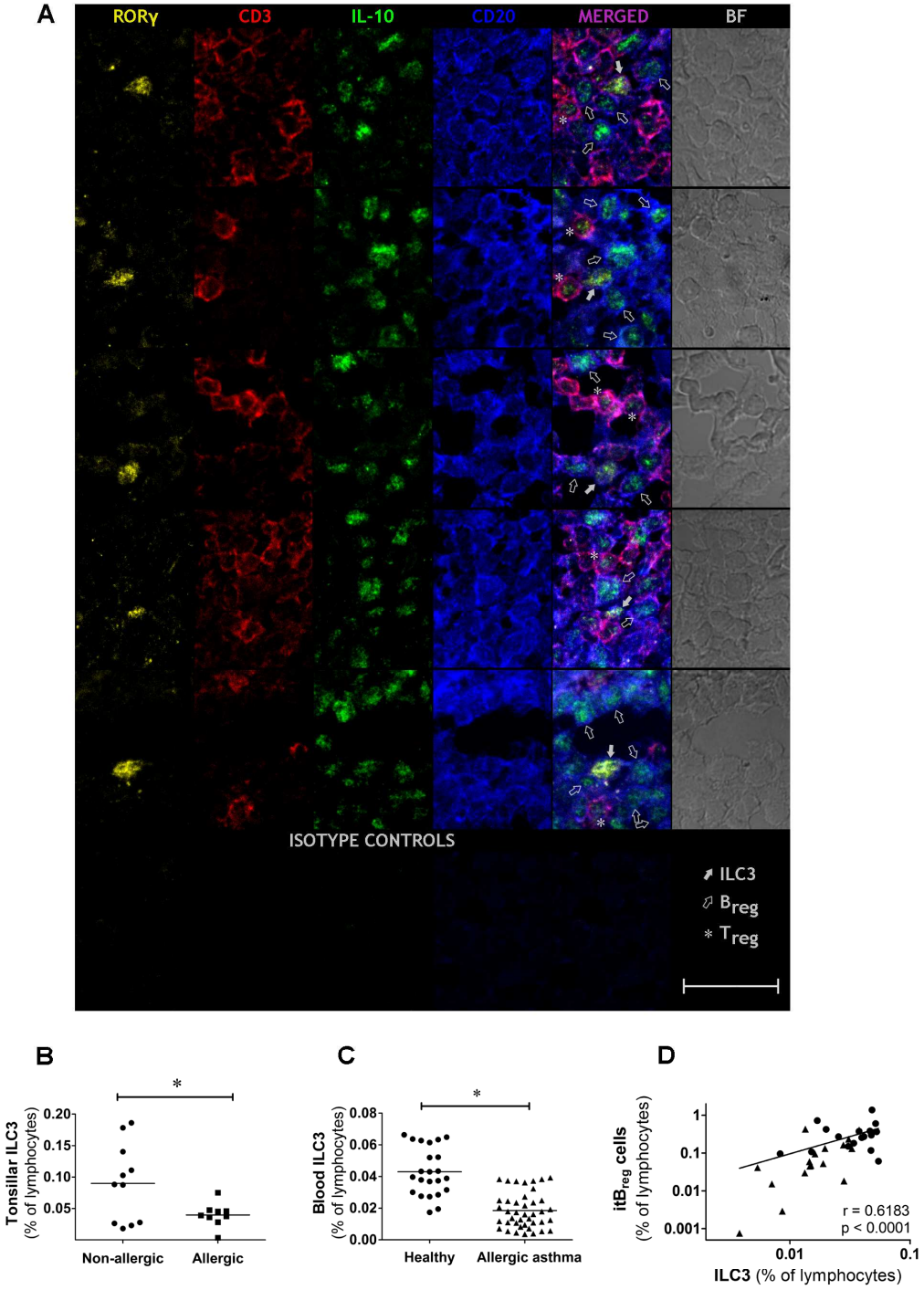

Figure 8 Komlósi ZI et al.

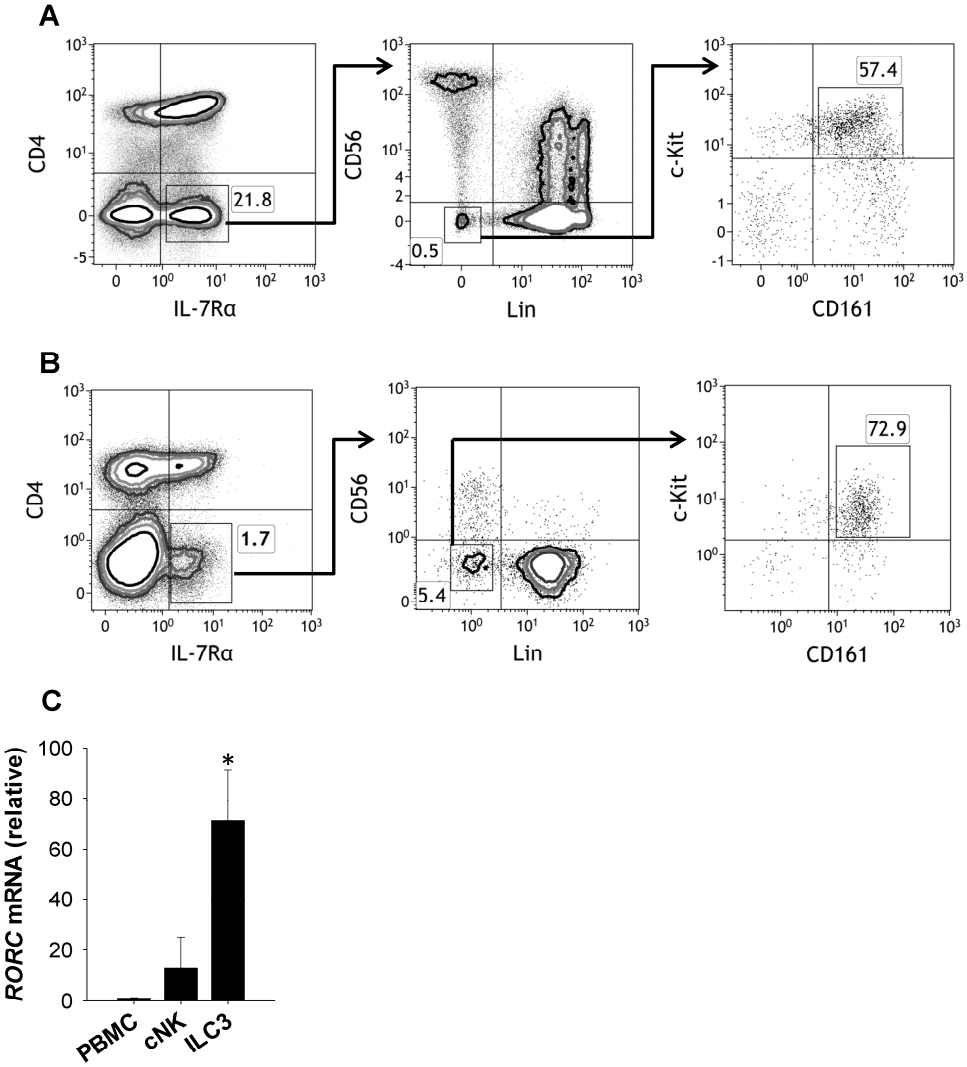

Figure E1 Komlósi ZI et al.

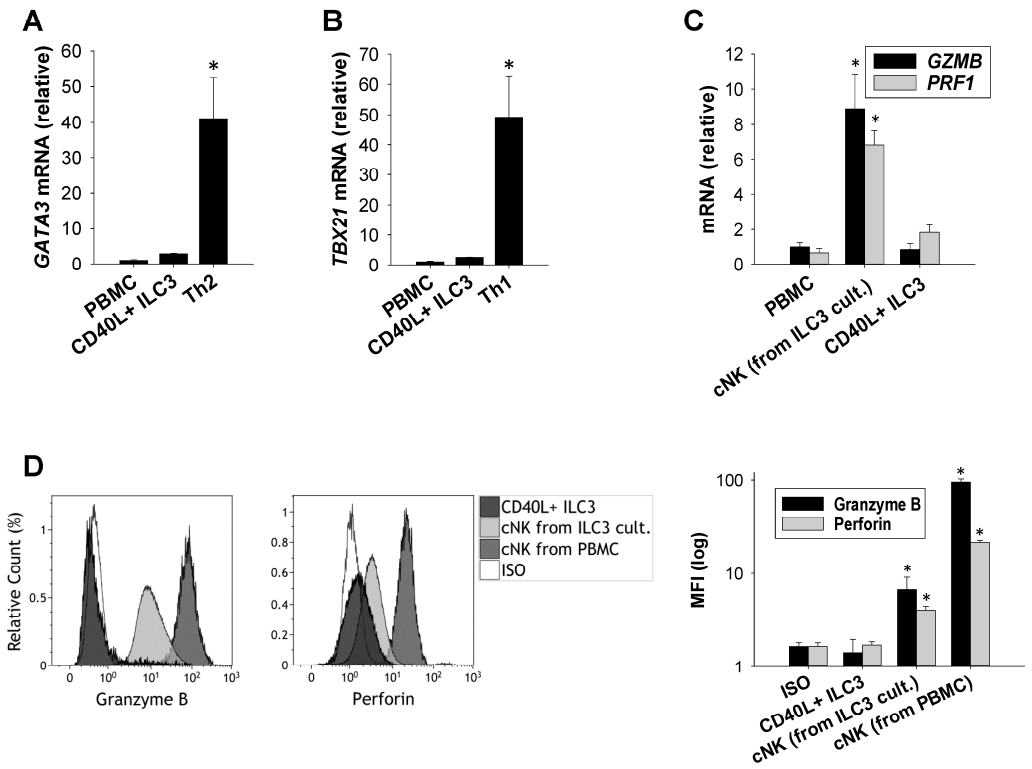

Figure E2 Komlósi ZI et al.

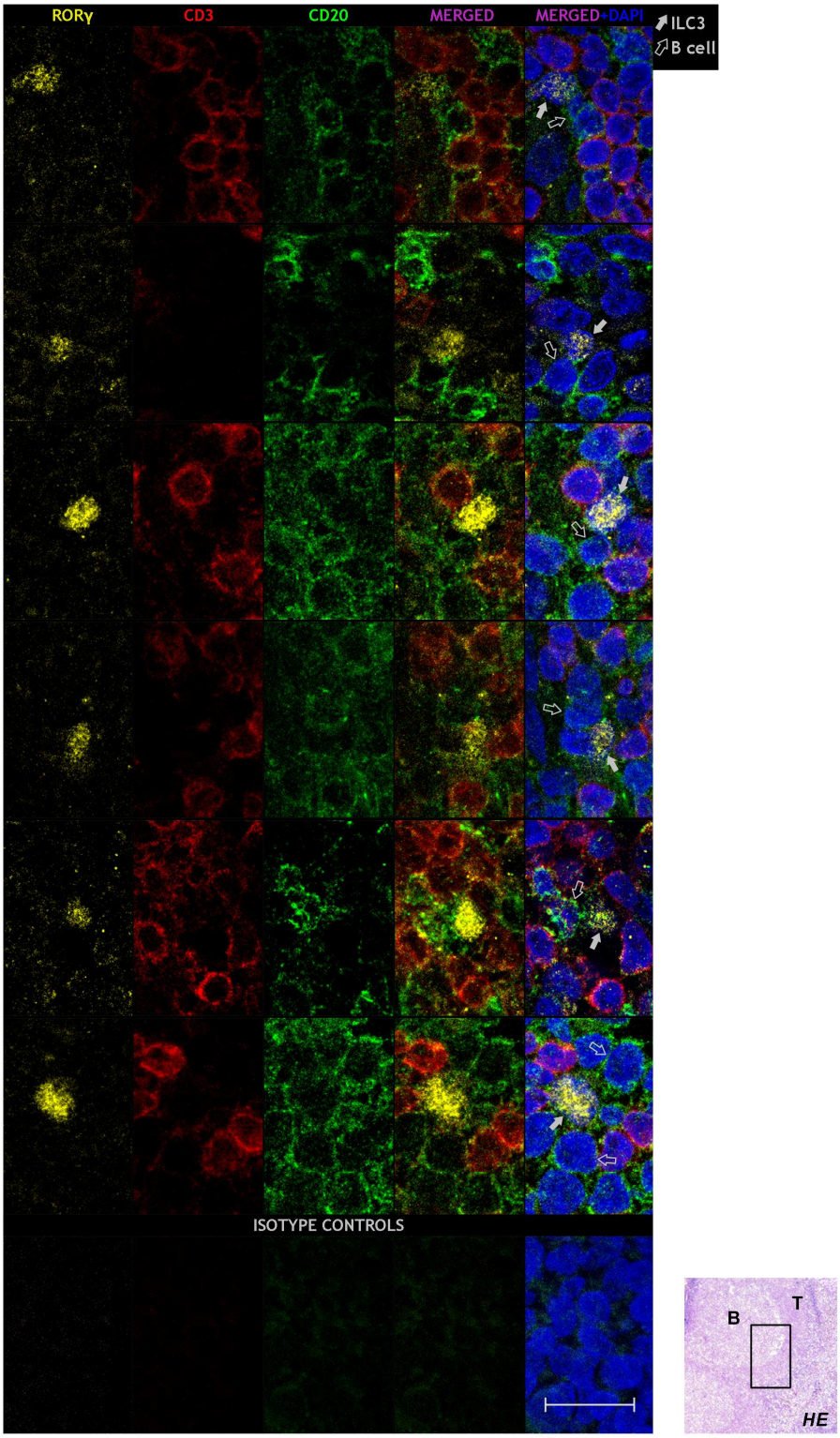

Figure E3 Komlósi ZI et al.

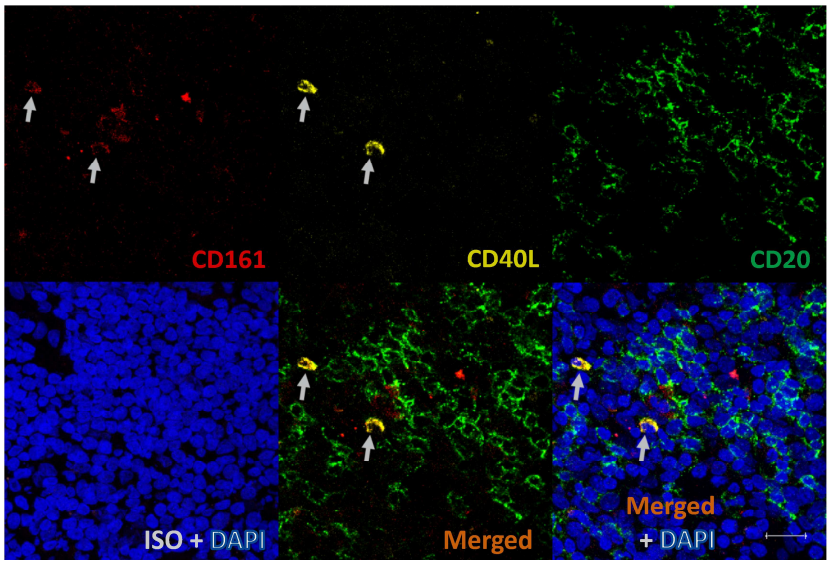

Figure E4 Komlósi ZI et al.

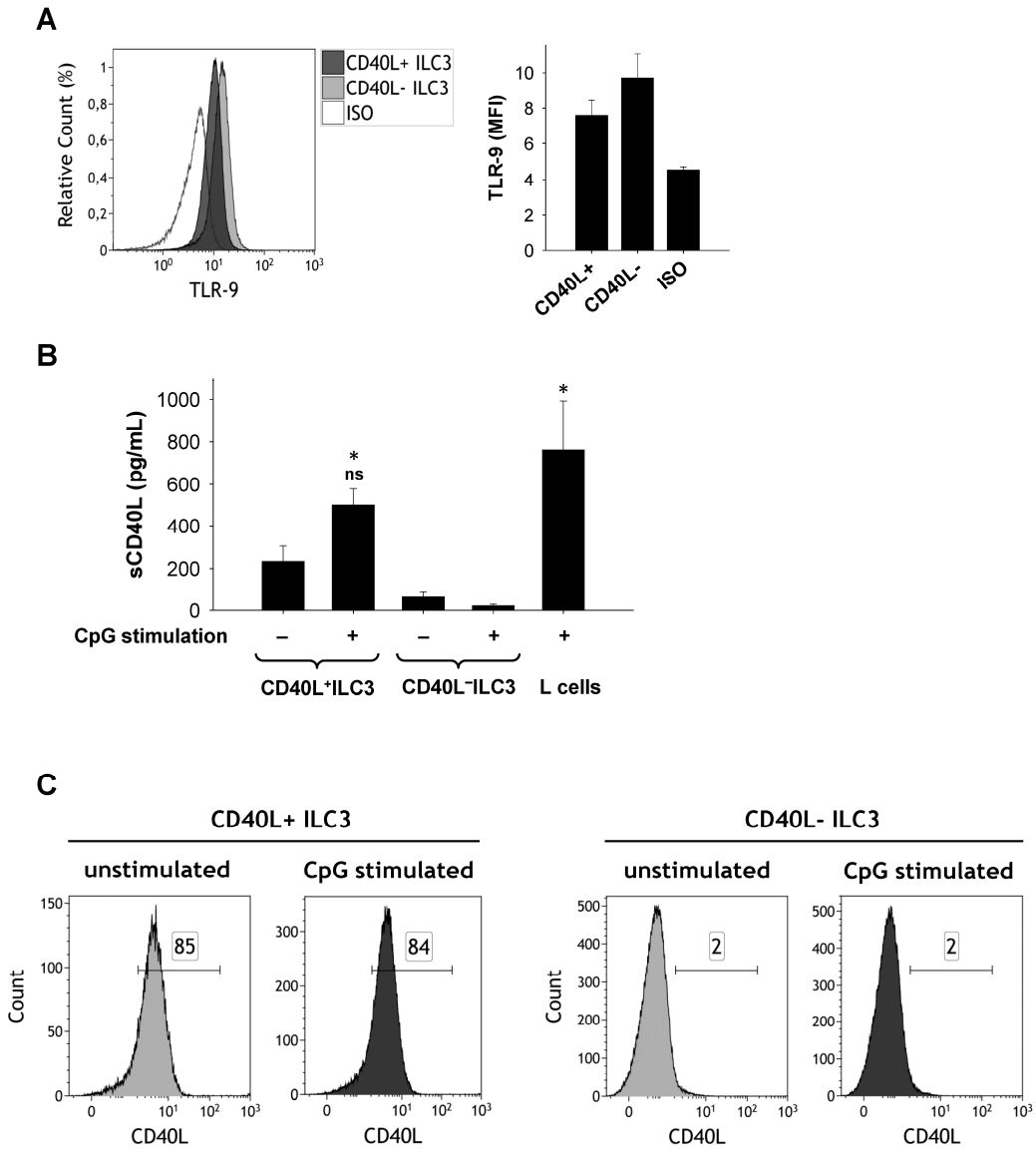

Figure E5 Komlósi ZI et al.

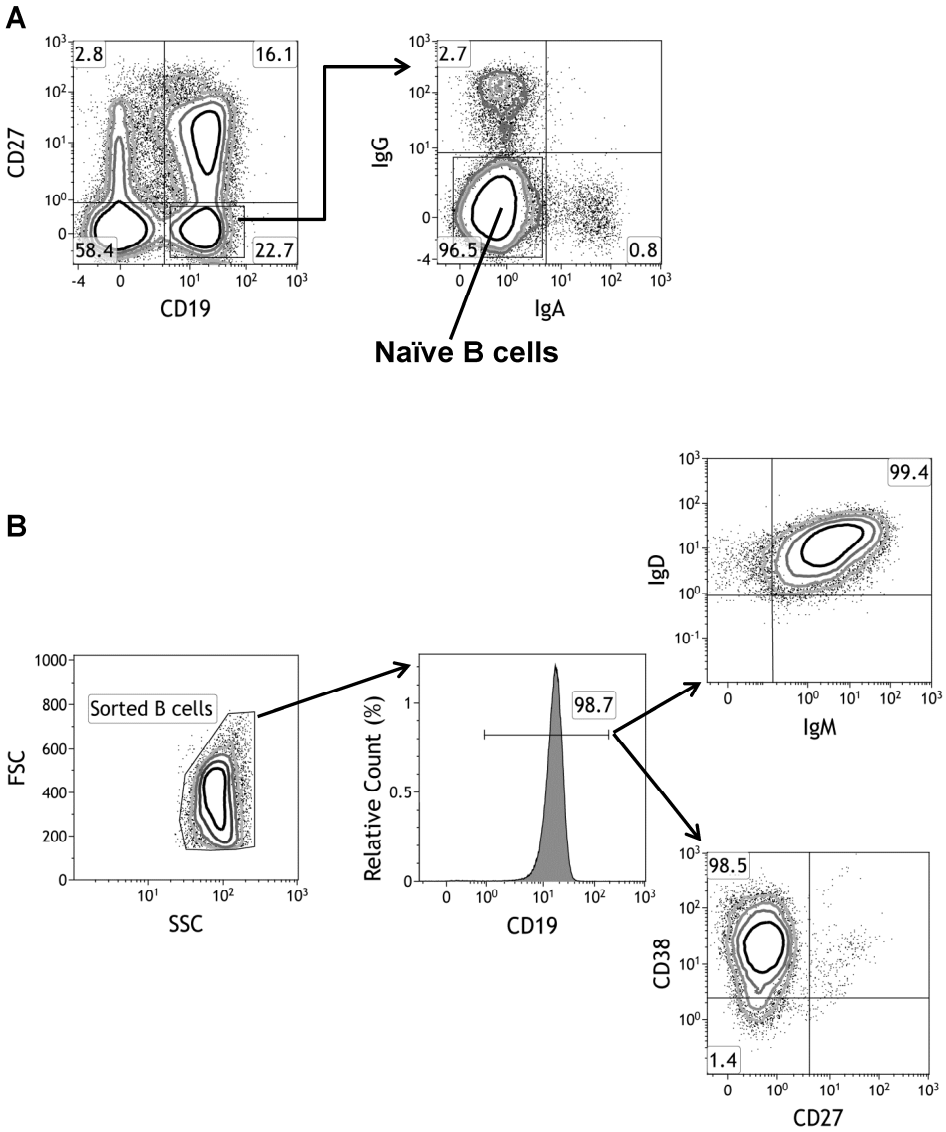

Figure E6 Komlósi ZI et al.

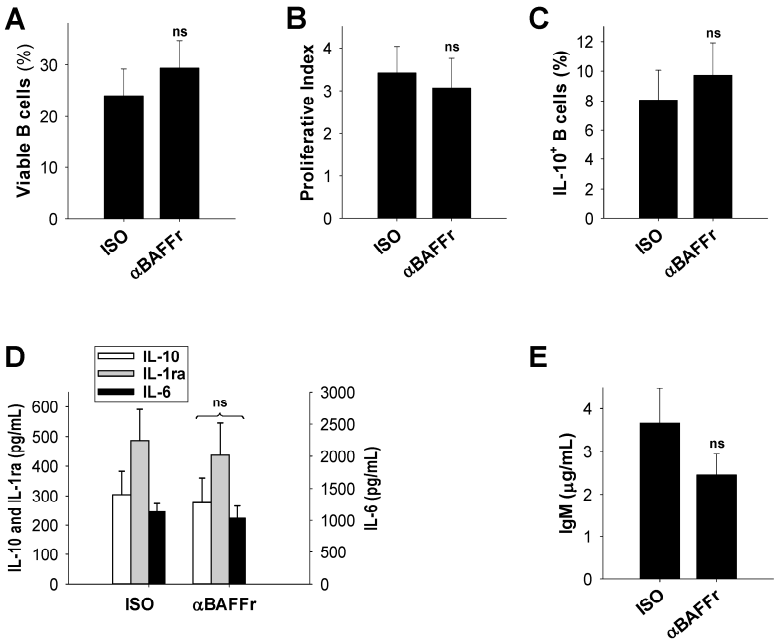

Figure E7 Komlósi ZI et al.

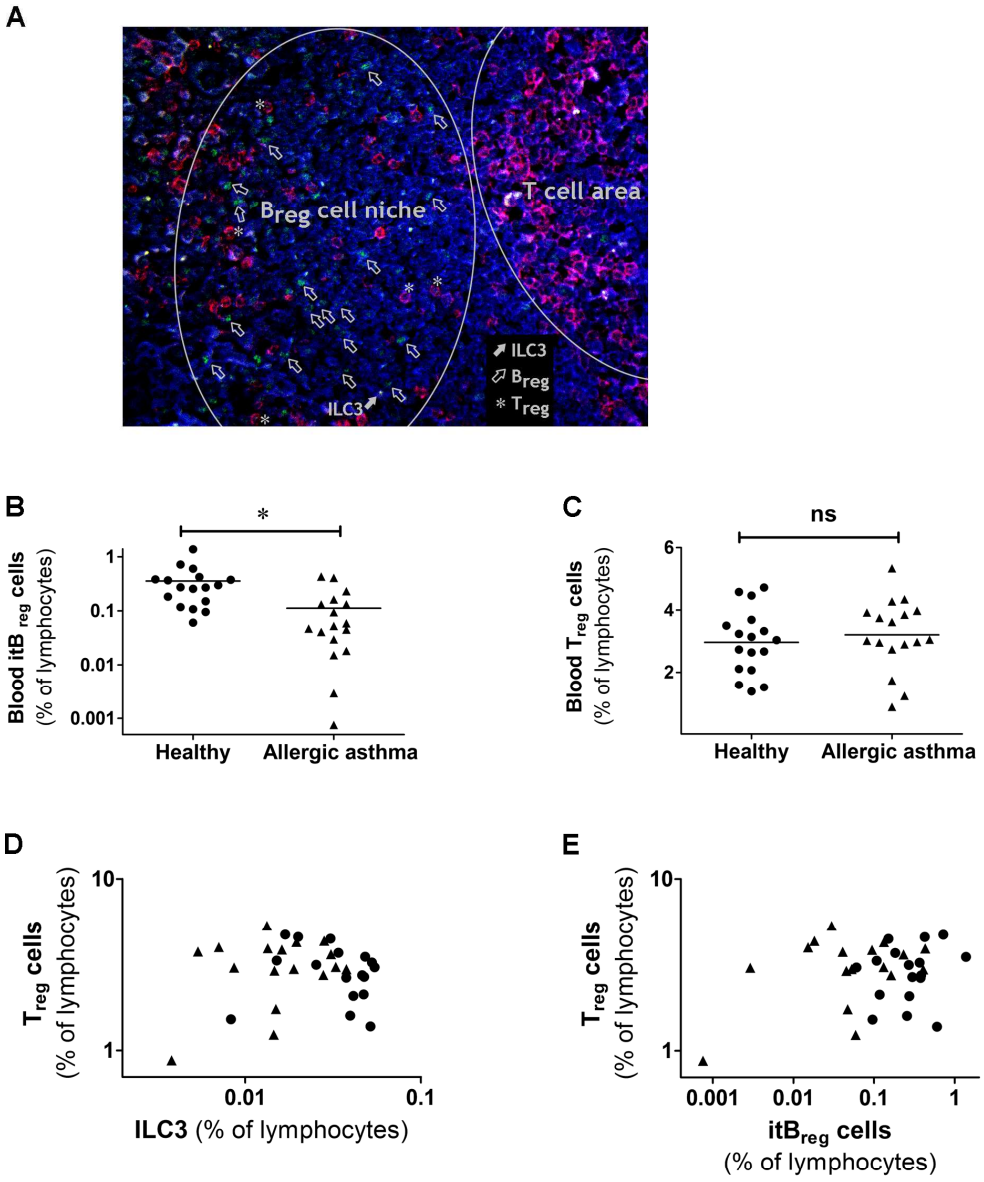

Figure E8 Komlósi ZI et al.

ONLINE REPOSITORY

MATERIALS AND METHODS

Isolation of cells

Peripheral blood mononuclear cells (PBMCs) were isolated by Ficoll (Biochrom) density gradient centrifugation within 3 hours of sample collection. Tonsil mononuclear cells (TMCs), tonsillar myeloid and plasmacytoid DCs (mDCs and pDCs) were isolated as previously described by us[40]. Briefly, single-cell suspensions of TMCs were isolated by mechanical disruption. The tissues were chopped and grounded with RPMI 1640 medium (Sigma) through a 40 μM mesh. After several washing steps with medium, the cells were purified by centrifugation on a Ficoll density gradient.

For tonsillar T cell and B cell preparation, TMC samples were labeled with magnetic microbead-bound anti-CD3 and anti-CD19 antibodies, respectively, and the positive cell populations were isolated by immunomagnetic separation.

Tonsil DCs were isolated from TMCs via negative selection by immunomagnetic separation (AutoMACS, Miltenyi Biotec) using magnetic microbead-bound anti-CD3, anti-CD19, anti-CD16, anti-CD14, and anti-CD326 antibodies in the presence of Fc-receptor-blocking reagent (Miltenyi Biotec). Tonsil mDCs were obtained from tonsil DCs via positive selection by CD1c (BDCA-1)$^+$ dendritic cell isolation kit (Miltenyi Biotec) supplemented in the first incubation step with anti-CD11c biotinilated antibody. The negative fraction was used for the isolation of tonsil pDCs via positive selection by CD304 (BDCA-4/ Neuropilin-1) microbead kit (Miltenyi Biotec).

Tonsillar epithelial cells were isolated according to a previously described protocol[E1]. Briefly, the epithelium were cut off the tonsil tissue, were cut into pieces of approximately 1-2 mm and trypsinized for 3 hours at 37℃ (Trypsin EDT A 0.05 %, Gibco). Trypsin was neutralized using TNS (Lonza) and the cells were filtered through a 40 μm nylon mesh. The obtained cells were seeded in 75 cm^2 plastic culture flasks and cultured in bronchial epithelial

growth medium (Lonza). Medium was changed after 24 hours and every second day from then on. Cells were harvested at a confluence of 90 % by trypsinisation.

Tonsillar T and B cell, DC and epithelial cell samples were used for *IL15* mRNA measurements.

For cryopreservation, TMCs were resuspended in freezing medium (10% DMSO and 45% fetal bovine serum in complete RPMI 1640) and stored in liquid nitrogen until flow cytometric measurements, as well as ILC3 and B cell isolations by fluorescence activated cell sorting.

Flow cytometry

For the ILC3 measurements, 2.5 million cells were acquired by flow cytometry. The minimum limit was 1 million cells. For readout measurements of the coculture experiments, 20'000-50'000 cells were measured.

Establishment of CD40L$^+$ILC3 cell line, as well as CD40L$^+$ILC3 and B cell cocultures

All cell cultures were grown in RPMI 1640 medium supplemented with 1 mM sodium pyruvate (Sigma), 1% MEM nonessential amino acids and vitamins (Sigma), 2 mM L-glutamine (Sigma), 100 U/ml penicillin, 100 µg/ml streptomycin (Sigma), 100 µg/ml kanamycin (Gibco) and 10% heat-inactivated FCS (Sigma). Cells were cultured in 96 well plates in 500-1000 cells/µL concentration.

L cells are mouse fibroblasts transfected with human CD40L, and are widely used as supporting cells in B cell experiments. L cells express high levels of human CD40L on their surface, and also releases soluble CD40L (sCD40L). Irradiated L cells (75 Gy) in 50,000/mL concentration were used as controls in our experiments in order to compare the supporting characteristics and performance of an artificial, highly optimized coculturing cell (L cell) to a biologically relevant cell type (CD40L$^+$ILC3). For T and B cell cocultures CD3$^+$CD4$^+$ T cells were sorted from the second blood sample of the same donor.

Proliferation and suppression assays

B cell proliferation was analyzed on (co-)culture day 12 by flow cytometric detection of carboxyfluorescein diacetate succinimidyl ester (CFSE; Invitrogen) dilution. Proliferative index is the median number of divisions the B cells have passed through since the beginning of the experiment. For ILC3 proliferation assay, we used Celltrace Violet (Molecular Probes), and analyzed on the same way. Cells were stimulated with IL-15, (10 ng/mL; from PeproTech). In suppression assay rhIL-10 (10 ng/mL from PeproTech) were used in the control wells. Autologous $CD3^+CD4^+CD25^+IL\text{-}7R\alpha^-$ regulatory T cells were sorted and used for control conditions in suppression assays.

Analysis of cytokine production, intracellular staining

Blood-derived $CD40L^+$ILC3s, $CD40L^-$ILC3s and cNK cells were cultured with IL-23 (50 ng/mL, 24h) for the IL-22-production assays; and $CD40L^+$ILC3s were cultured with IFN-γ (0.1 µg/mL, 2 days) for the BAFF expression experiments (all human recombinant cytokines were from PeproTech). IL-22 production of the ILC3s and cNK cells (in response to IL-23) was measured after 6 h of phorbol myristate acetate (PMA; 25 ng/ml; Sigma) and ionomycin (1 µg/mL; Sigma) stimulation with ELISA (PeproTech). Tonsil-derived naïve B cells were stimulated with CpG (1 µM) and or BAFF (2 µg/mL) for 4 days in order to induce IL-15 production.

Cytofix/Cytoperm Fixation and Permeabilization Kit (Beckton Dickinson) were used for cell permeabilization and intracellular staining procedure both for the staining of cytokines (IL-10, IL-6, IL-15) and for the other intracellular stainings (TLR-9, Granzyme B, Perforin). For the intracellular IL-10, IL-6 and IL-15 staining, cells were stimulated with PMA (25 ng/ml; Sigma) and ionomycin (1 µg/mL; Sigma) for 6 h in the presence of brefeldin A (10 µg/ml; Sigma) for the final 2 h. For intranuclear transcription factor (RORγt) staining in blood-derived $CD40L^+$ILC3s, $CD40L^-$ILC3s and cNK cells a Fix/Perm Buffer Set and a corresponding Cell Staining Buffer (Biolegend) were used. Data were acquired on Galios (Beckman Coulter) flow cytometer, and were analyzed with Kaluza software (Beckman Coulter).

Analysis of cytokine and immunoglobulin production

Production of cytokines (IL-10, IL-1ra, IL-6, sCD40L) and IgM were measured in cell culture supernatants by multiplex cytometric bead-based immunoassays (Bio-Plex system, Bio-Rad). Supernatants of various cultures were harvested on day 6 for the cytokine, and on day 12 for the immunoglobulin measurements. Spontaneous cytokine and immunoglobulin secretion of the cells after the initial (day 1) CpG stimulation were detected, and it was not boosted by any further stimulation.

Quantitative real-time RT-PCR

Total RNA was extracted with RNeasy Micro kit (Qiagen) according to the manufacturer's instructions. cDNA was synthesized using oligo-dT and reverse transcription reagents (Thermo Scientific) according to manufacturer's protocols. SYBR Green/ROX qPCR master mix (Bio-Rad) was used for amplification of the PCR products. All primers were designed by us (listed in **Supplementary Table 1.**; purchased from Microsynth). Quantitative RT-PCR analysis was carried out on ABI Prism 7900HT instrument (Applied Biosystems), the relative gene expression levels were calculated using the comparative Ct ($\Delta\Delta C$t) method. All results were normalized to the expression of *EEF1A1* (encoding elongation factor 1α).

Immunofluorescence histology

The preparation, staining procedure and acquisition of frozen human palatine tonsil tissue sections were previously described by us[41]. Briefly, palatine tonsil tissues were embedded in Optimal Cutting Temperature (OCT) *compound* (Tissue-Tek, Sakura Finetek), frozen in liquid nitrogen-cooled 2-methylbutane (Fluka), and stored at -80℃ until cryosections were cut by an HM 500 OM Cryostat microtome (Mikrotom). Paraformaldehyde-fixed cryosections (7 µm) were sequentially incubated with the primary antibody, an Alexa Fluor dye-conjugated goat secondary antibody, and blocked with the isotype control antibody corresponding to the primary antibody. These staining cycle were repeated with all subsequent primary antibodies

during the staining protocol. We developed a 4 color immunnofluorescence staining for the detection RORγt^{+}CD3^{-} ILC3s and CD20^{+}IL-10^{+} B_{reg} cells together in the same specimen. The detection of ILC3s based on a previously reported approach[E2].

The following antibodies were used for the detection of ILCs in the tissue: anti-RORγt (AFKJS-9; eBioscience) anti-CD161 (DX12; Beckton Dickinson), anti-CD3 (CD3-12; Abd Serotec), anti-CD40L (40804; RnD), anti-CD20 (EP459Y; Epitomics), anti-IL-10 (polyclonal goat, RnD) and corresponding isotype control antibodies (from the same sources or Dako). Alexa Fluor dye-conjugated, species and isotype specific secondary antibodies (Invitrogen) were used for detection of the bound primary antibodies.

Tissue sections were mounted with ProLong Gold antifade reagent with or without DAPI (Invitrogen). Images were captured using a Leica TSC SPE confocal microscope with a ACS APO 63X 1.3 OIL objective. Data were acquired by *Leica Application Suite Advance Fluorescence 2.4.1* software (Leica Microsystems). Brightness, contrast and color balance of the pictures were adjusted in Imaris 7.7 image analysis software (Bitplane). Image panels were composed in Photoshop CS2. The general histology of palatine tonsils was demonstrated by staining of the sections with Hematoxylin and Eosin.

Antibodies and viability dye

The following antibodies were used for flow cytometric measurements and sorting experiments: Alexa Fluor 488-conjugated anti-CD24 (ML5), anti-IL-7Rα (anti-CD127; A019D5), fluorescein isothiocyanate (FITC)-conjugated anti-IL-6 (MQ2-13A5), phycoerythrin (PE)-conjugated anti-BAFF (T7-241), anti-CD138 (DL-101), anti-CD94 (DX22), anti-IgD (IA6-2), anti-IL-6 (MQ2-13A5), PE/Dazzle594-conjugated anti-CD38 (HIT2) peridinin chlorophyll protein-cyanine 5.5 (PerCP-Cy5.5)-conjugated anti-CD3 (UCHT1), anti-CD19 (HIB19), anti-CD20 (2H7), anti-CD14 (HCD14), anti-CD11c (B-ly6), anti-CD34 (581), anti-CCR6 (TG7/CCR6), anti-IgM (MHM-88), PE-indotricarbocyanine (Cy7)-conjugated anti-CD1d (51.1), anti-c-Kit (anti-CD117; 104D2), anti-CD38 (HIT2), allophycocyanin (APC)-conjugated anti-CD161 (HP-3G10), anti-CD94 (DX22), Alexa Fluor 647-conjugated anti-IL-10 (JES3-

9D7), Alexa Fluor 700-conjugated anti-CD19 (HIB19), APC-Cy7-conjugated anti-CD19 (HIB19), anti-CD40L (anti-CD154; 24-31), IgM (MHM-88), Pacific Blue (PB)-conjugated anti-CD56 (MEM-188), Brillant Violet (BV) 421-conjugated anti-CD24 (ML5), anti-c-Kit (anti-CD117; 104D2), BV510-conjugated anti-CD19 (HIB19) and isotype-matched control antibodies conjugated to PE, PB, Alexa Fluor 700, APC-Cy7, BV421 and BV510 (MOPC-21), conjugated to FITC, PE (RTK2071), and conjugated to BV421 (MOPC-173; all from BioLegend); FITC-conjugated anti-IL-7Rα (anti-CD127; HIL-7R-M21), anti-PD-L1 (CD274; MIH1), anti-IgD (IA6-2), PE-conjugated anti-CD3 (HIT3A), anti-CD40L (anti-CD154; TRAP1), anti-CD27 (M-T271), PerCP-Cy5.5-conjugated anti-CD3 (UCHT1), anti-CD14 (M5E2), anti-CD56 (B159), APC-conjugated anti-CD161 (DX12), anti-CD40L (anti-CD154; TRAP1), Alexa Fluor 647-conjugated anti-NKp44 (p44-8.1), and isotype-matched control antibodies conjugated to FITC, Alexa Fluor 488, PE, PerCP-Cy5.5, PE-Cy7, Alexa Fluor 647, APC (MOPC-21; all from Beckton Dickinson); PE-conjugated anti-RORγt (AFKJS-9), anti-Granzyme B (GB11), anti-Perforin (dG9), anti-CD1d (51.1), anti-TLR-9 (eB72-1665), and isotype-matched control antibodies conjugated to PE (rat IgG2a - eBR2a and mouse IgG2a - eBMG2b; all from eBioscience); PE-conjugated anti-CD56 (N901 (NHK-1)), anti-IgD (IADB6), PE-Texas Red-conjugated anti-CD4 (SCFCI12T4D11), APC-AF750-conjugated anti-CD3 (UCHT1), and isotype-matched control antibodies conjugated to PE-Texas Red (2T8-2F5), APC-AF750 (679.1Mc7; all from Beckman Coulter); PE-conjugated and APC-conjugated anti-IL-15 (34559), purified anti-APRIL (670840; all from R&D Systems); Alexa Fluor 647-conjugated goat anti-mouse IgG secondary antibody (polyclonal, from Invitrogen); Alexa Fluor 488-conjugated anti-IgG and Alexa Fluor 647-conjugated anti-IgA (policlonal goat antibodies, both from Jackson ImmunoResearch).

Fixable viability dyes (eFluor 450 and eFluor 780, eBioscience; termed as e-450 and e-780) was used for dead cell discrimination. We used two different viability dyes to fit them in the best way to various multicolor ILC3 and B cell flow cytometry panels.

For functional experiments the following neutralizing and isotype control antibodies were used: purified (low endotoxin, azide free) anti-CD40L (anti-CD154; 24-31), anti-IL-10R

(3F9) and isotype matched control antibodies (MOPC-21, RTK2758; all from Biolegend); anti-BAFFr/TNFRSF13C and normal IgG control polyclonal goat antibodies (both from R&D Systems).

REFERENCES

E1. Soyka MB, Wawrzyniak P, Eiwegger T, Holzmann D, Treis A, Wanke K, et al. Defective epithelial barrier in chronic rhinosinusitis: the regulation of tight junctions by IFN-gamma and IL-4. J Allergy Clin Immunol 2012; 130:1087-1096 e1010.

E2. Kim S, Han S, Withers DR, Gaspal F, Bae J, Baik S, et al. CD117(+) CD3(-) CD56(-) OX40Lhigh cells express IL-22 and display an LTi phenotype in human secondary lymphoid tissues. Eur J Immunol 2011; 41:1563-1572.

FIGURES

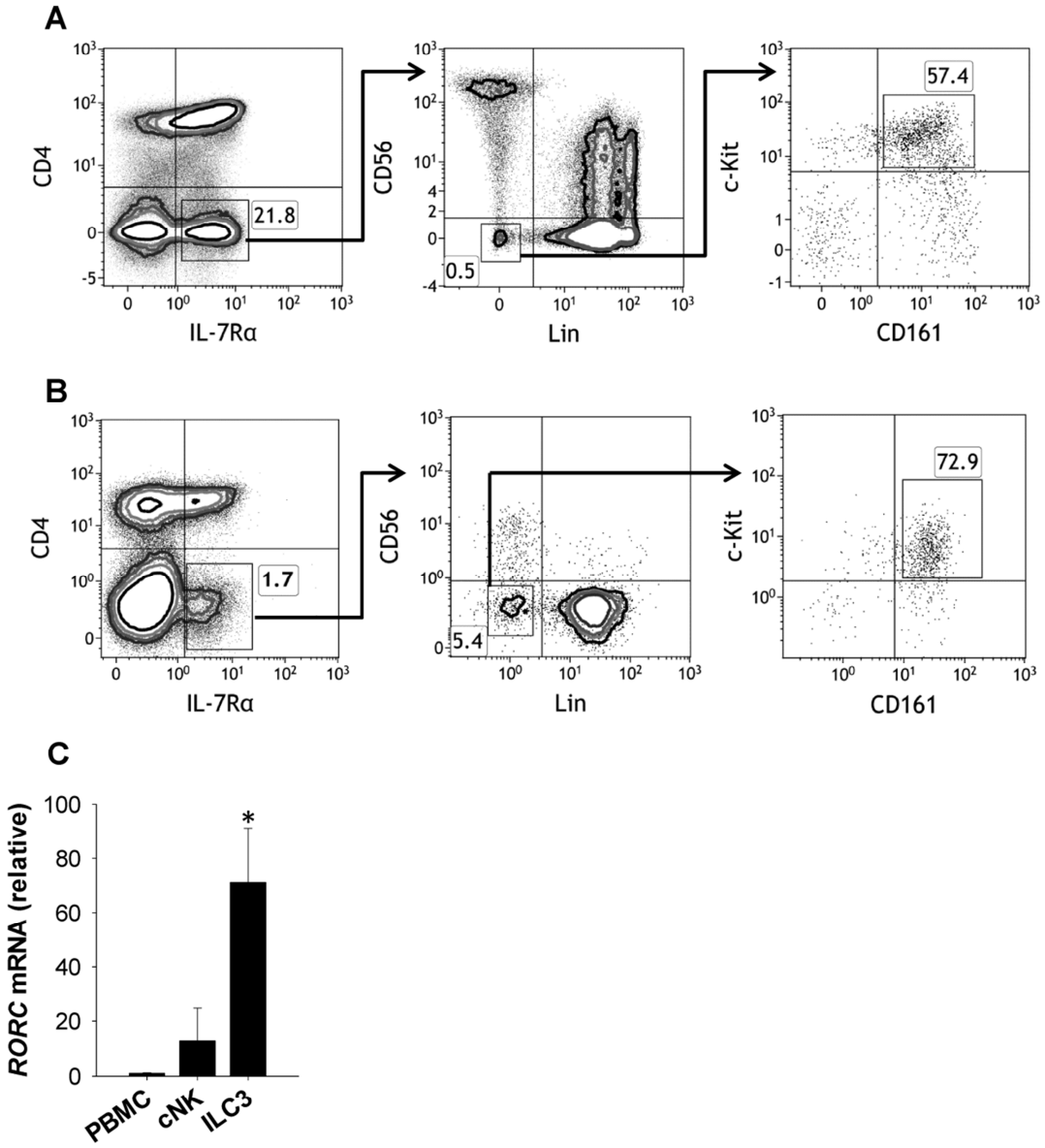

FIG E1.

Type 3 innate lymphoid cells (ILC3s) in peripheral blood and tonsil tissue

(**A**) Flow cytometric analysis of the ILC3s in peripheral blood mononuclear cells (PBMCs). First plot is gated on lymphocytes identified by size and complexity. Lineage markers (Lin) were CD3, CD19, CD20, CD14, CD34, CD11c, CD94. Numbers indicate percent cells in parent gate. ILC3s defined as IL-7Rα^{+}CD4^{-}Lin^{-}CD56^{-}CD161^{+}c-Kit^{+} cells. Data are representative of more than fifty independent experiments.

(**B**) Flow cytometric analysis of the ILC3s in tonsillar mononuclear cells (TMCs). First plot is gated on lymphocytes identified by size and complexity. Data are representative of twelve independent experiments.

(**A**) and (**B**) ILC3s were sorted from PBMC and TMC samples with FACSAria II (Beckton Dickinson) according to the gating strategy shown on **A** and **B**, respectively.

(**C**) *RORC* mRNA expression of freshly isolated blood ILC3s. Total PBMCs and sorted cNK cells were controls (*: $p<0.05$ vs PBMC and cNK; mean ± SEM; n=5, one-way ANOVA with Bonferroni *post hoc* test).

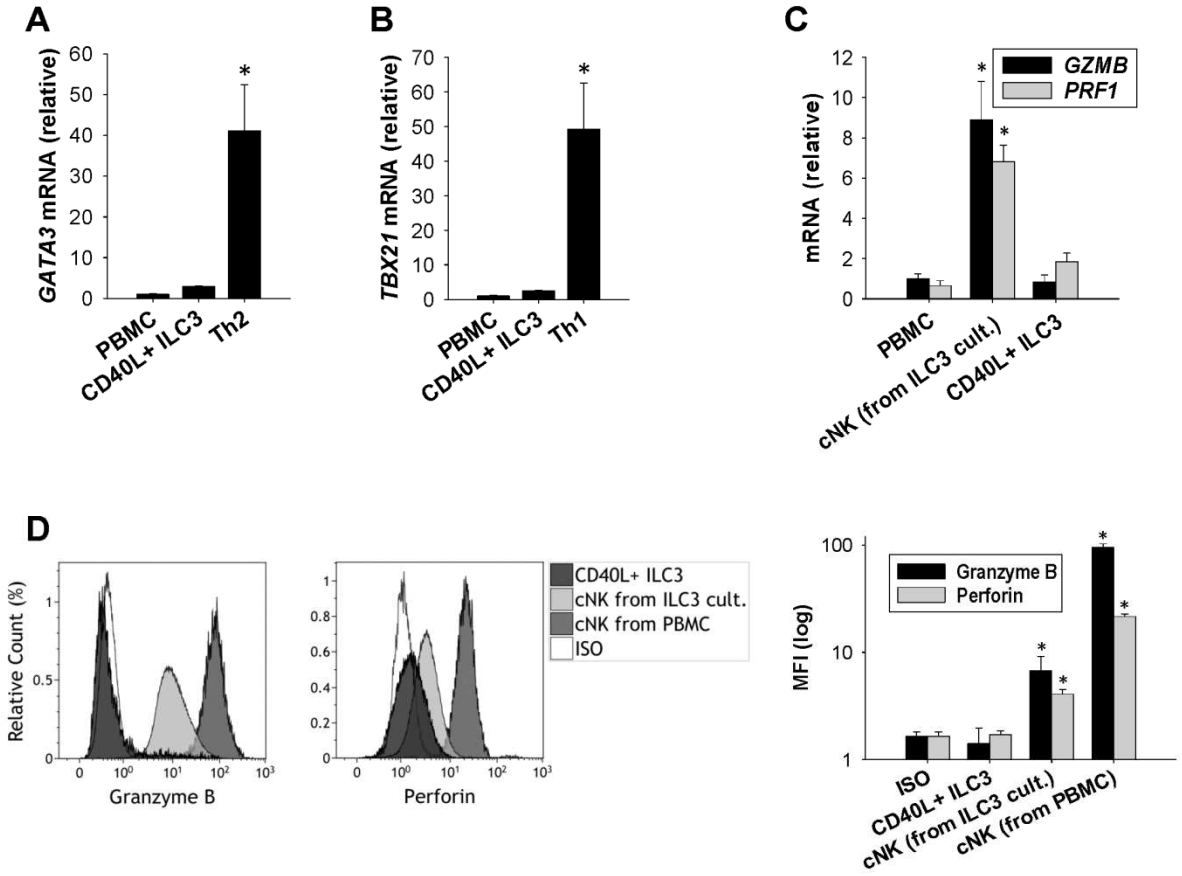

FIG E2.

The new expansion strategy with IL-15 results in ILC3s clearly distinct from ILC2s, ILC1s and cNK cells.

(**A-D**) CD40L^{+}ILC3s did not show the characteristics of ILC1, ILC2 or cNK cells.

(**A**) and (**B**) Lack of *GATA3* (**A**) and *TBX21* (**B**) mRNA expression of CD40L^{+}ILC3s sorted according to the gating strategy shown on **Fig. 1A**. *TBX21* gene is encoding T-bet. Total PBMCs and *in vitro* differentiated Th2 (**A**) and Th1 (**B**) cells were used as controls (*: $p<0.01$ vs PBMC and CD40L^{+}ILC3).

(**C**) CD40L^{+}ILC3s did not express *GZMB* and *PRF1* mRNA encoding the cytotoxic enzymes granzyme B and perforin, respectively. CD40L^{+}ILC3s and cNK cells (from ILC3 cultures) were sorted according to the gating strategy shown on **Fig. 1A**. Freshly sorted peripheral blood cNK cells were used as controls (*: $p<0.05$ vs PBMC and CD40L^{+}ILC3).

(**D**) Intracellular granzyme B and perforin proteins were detected by flow cytometry. $CD40L^+$ILC3s and cNK cells (from ILC3 cultures) were sorted according to the gating strategy shown on **Fig. 1A**. Freshly isolated, blood-derived $CD56^{low}CD3^-$ cNK cells were used as positive controls (*: $p<0.05$ vs ISO and $CD40L^+$ILC3; MFI: median fluorescence intensity).

Mean ± SEM; (**B-E**) n=3-5, one-way ANOVA with Bonferroni *post hoc* test.

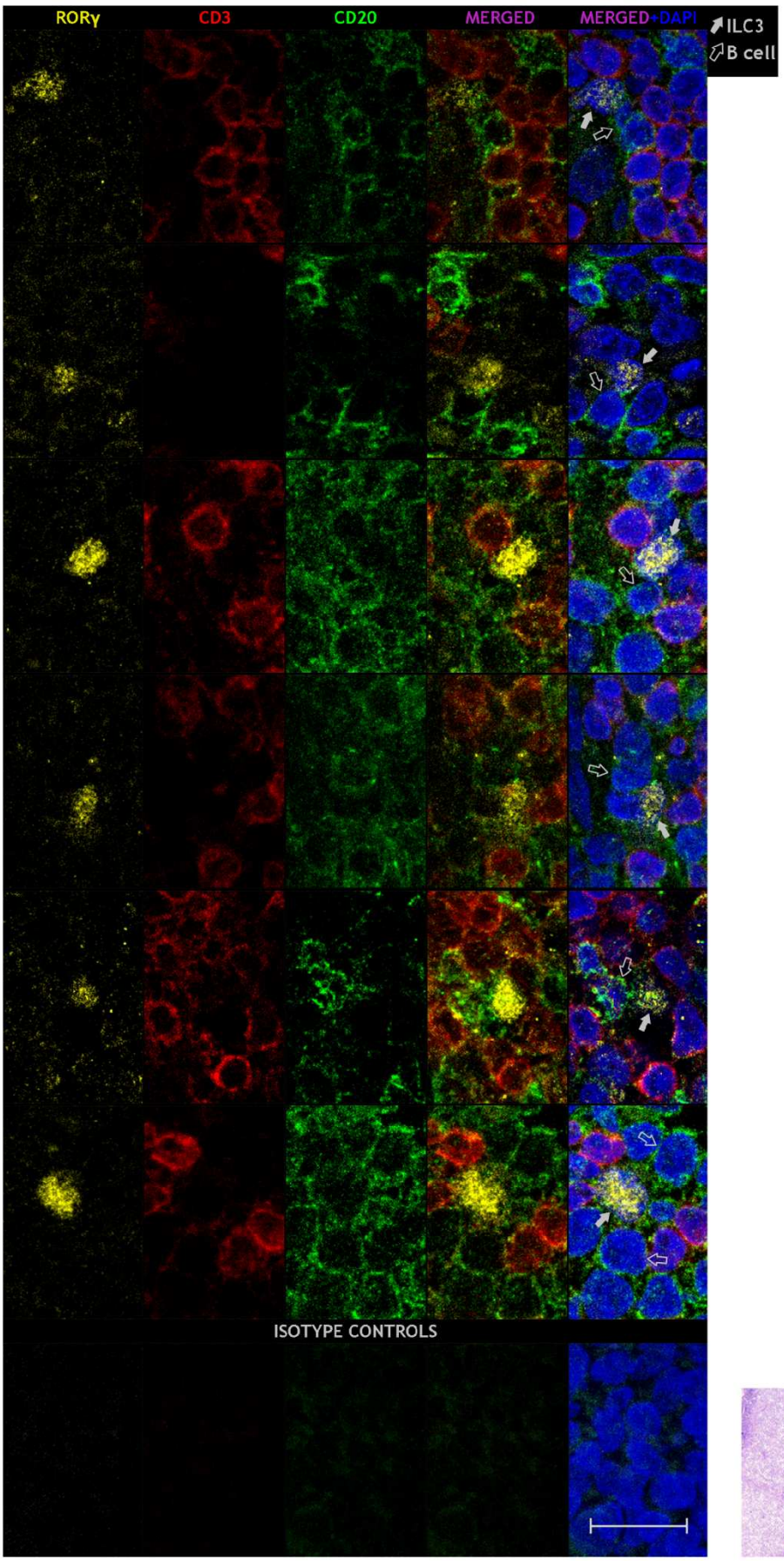
RORγ
CD3
CD20
MERGED
MERGED+DAPI
ILC3
B cell
ISOTYPE CONTROLS

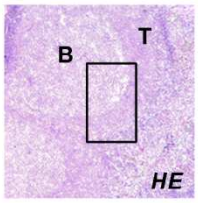
B
T
HE

FIG E3.

RORγt$^+$ ILC3s are residing at the interface between T and B cell areas in the tonsils, and are in close connection with B cells

Immunofluorescence histology of tonsils. The connection of RORγt$^+$CD3$^-$ ILC3s and B cells is demonstrated with a collection of pictures from different sections because the ILC3s are rare cells and scattered around the interface of the T and B cell areas in tonsils. Filled arrows: RORγt$^+$CD3$^-$ ILC3s. Open arrows: CD20$^+$ B cells. Representative isotype control stainings are shown in the lower row. In lower left corner the light microscopic structure of the tonsils is shown with Hematoxylin and Eosin staining. The B cell follicles ("B") are surrounded by the T cell area ("T"). The black quadrant approximately shows the field, which is magnified on immunofluorescence images.

Representative images of three independent experiments. Scale bar is 20 μm.

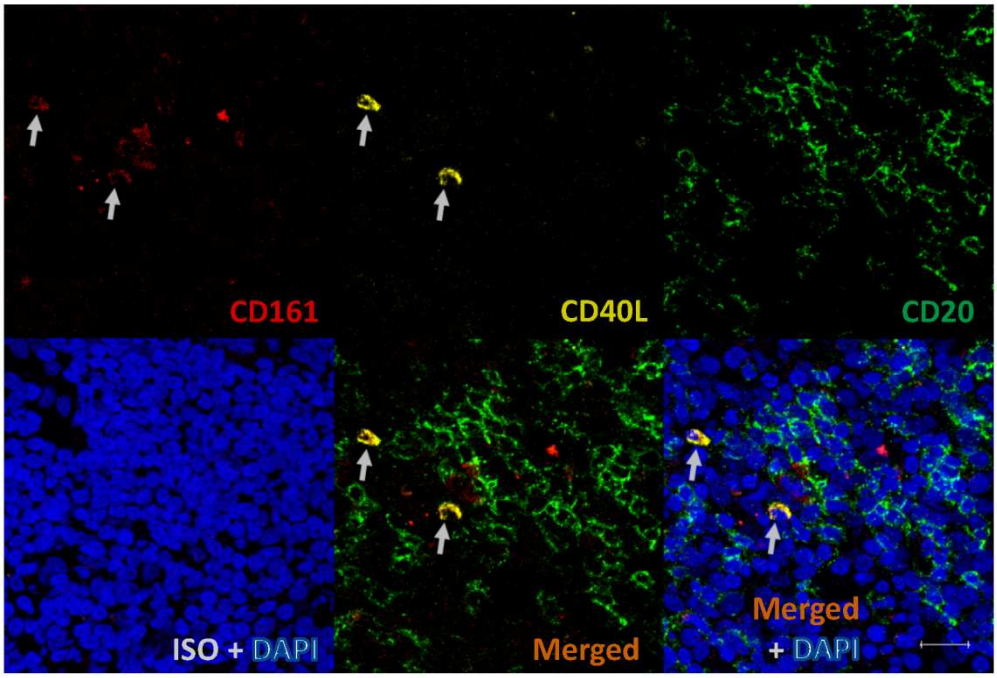

FIG E4.

CD40L^{+} ILCs are residing at the interface between T and B cell areas in the tonsils

Immunofluorescence histology of tonsils. Arrows show CD161^{+} CD40L^{+} and CD20^{-} ILCs on the border of the T cell - B cell areas in the tonsil tissue. CD40L^{+}ILCs are close to CD20^{+} B cells in tonsils.

Representative images of three independent experiments. Scale bar is 20 μm.

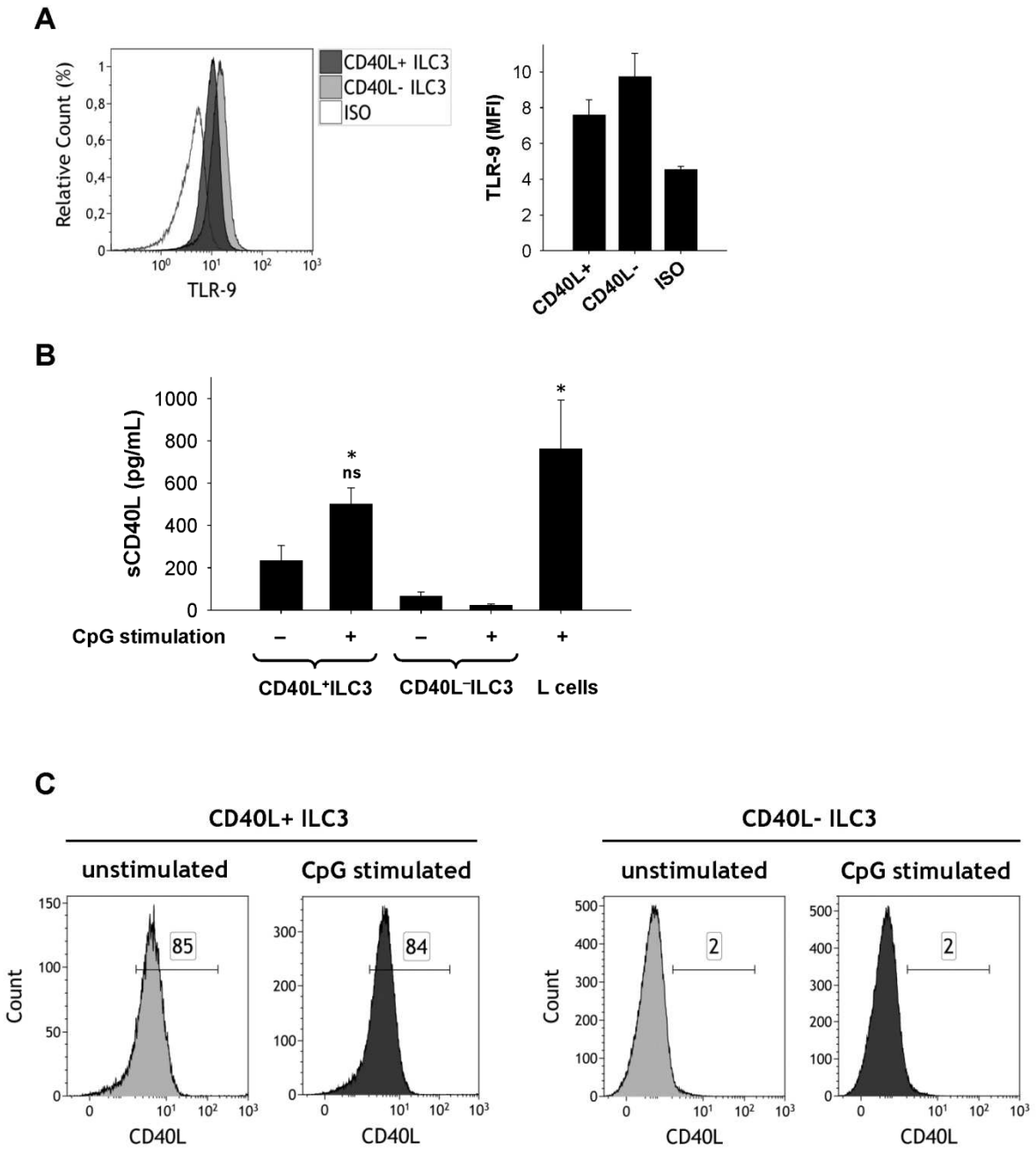

FIG E5.

TLR-9 and CD40L in ILC3s

(**A**) Intracellular toll-like receptor 9 (TLR-9) expression in $CD40L^{+}$ILC3s or $CD40L^{-}$ILC3s analyzed by flow cytometry (n=5).

(**B**) Soluble CD40L (sCD40L) concentrations were measured in supernatants of $CD40L^{+}$ILC3s alone, $CD40L^{-}$ILC3s alone and L cells alone cultures by multiplex bead assay,

with or without initial CpG stimulation. Equal numbers of $CD40L^{+}$ILC3s or $CD40L^{-}$ILC3s were seeded, and the supernatants were harvested on day 5 (*: $p<0.01$ vs $CD40L^{+}$ILC3 without CpG stimulation and all $CD40L^{-}$ILC3 cultures; ns: $p>0.05$ vs L cells with CpG stimulation; one-way ANOVA with Bonferroni *post hoc* test; n=5).

(**C**) The stability of CD40L expression on $CD40L^{+}$ILC3s or $CD40L^{-}$ILC3s after 8 days of culture with or without CpG stimulation, analyzed by flow cytometry. Data are representative of 2 independent experiments.

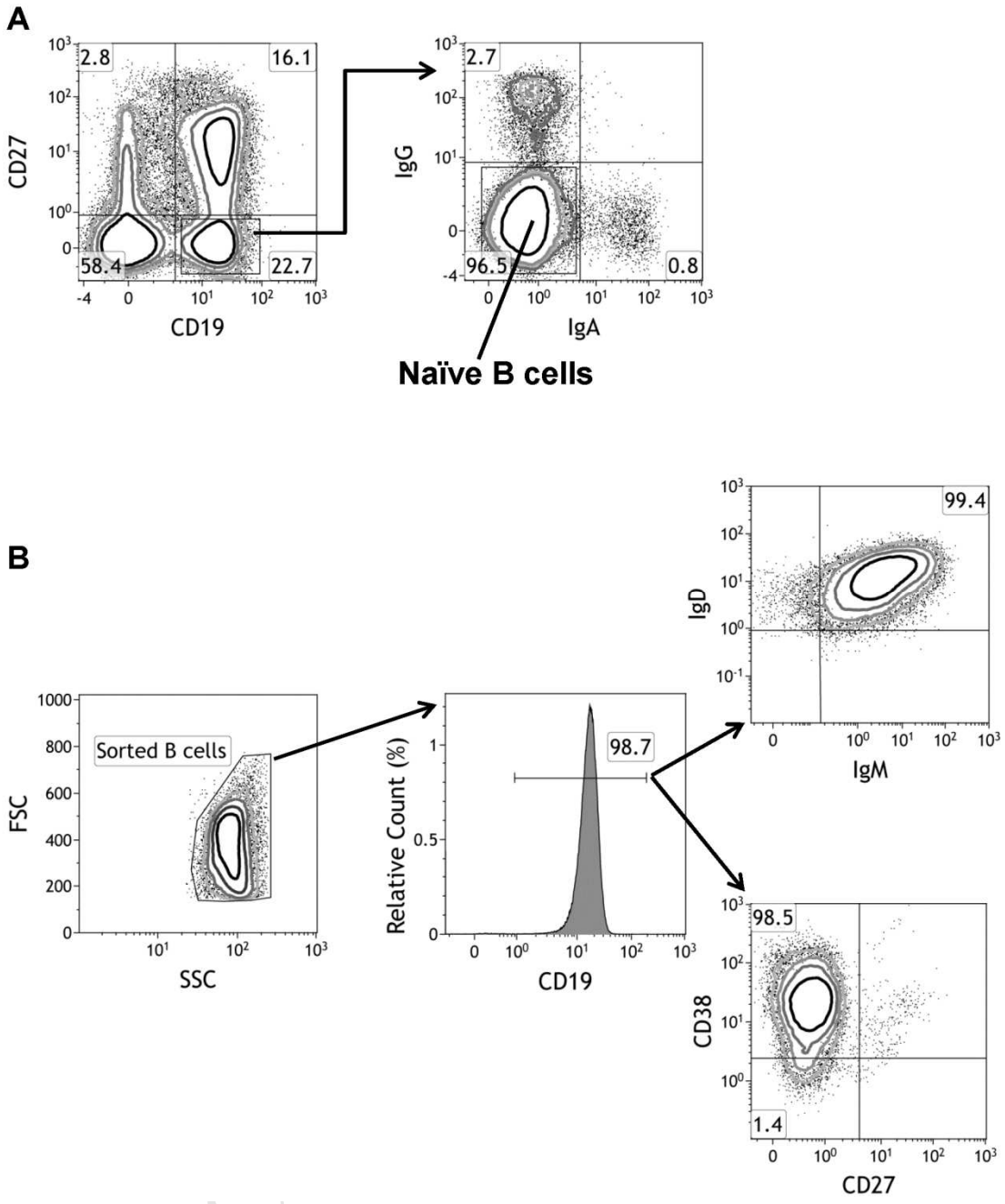

FIG E6.

Naïve B cells isolation strategy and purity check of the sorted cells

(**A**) Sorting strategy for circulating naïve B cells isolation. These cells were used for the blood-derived ILC3 and B cell cocultures. First plot is gated on peripheral blood lymphocytes identified by size and complexity (PBMCs were used as a sample). Naïve B cells were defined as $CD19^{+}CD27^{-}IgG^{-}IgA^{-}$ cells. We used the same isolation strategy for tonsillar

naïve B cell isolation also. Tonsillar naïve B cells were isolated from TMC samples and used for the tonsil-derived ILC3 and B cell coculture experiments.

(**B**) The sorted naïve B cell purity was examined by flow cytometry. The isolated naïve B cells were highly pure $CD19^{+}CD27^{-}IgD^{+}IgM^{+}CD38^{+}$ B cells.

Data are representative of fifteen independent experiments.

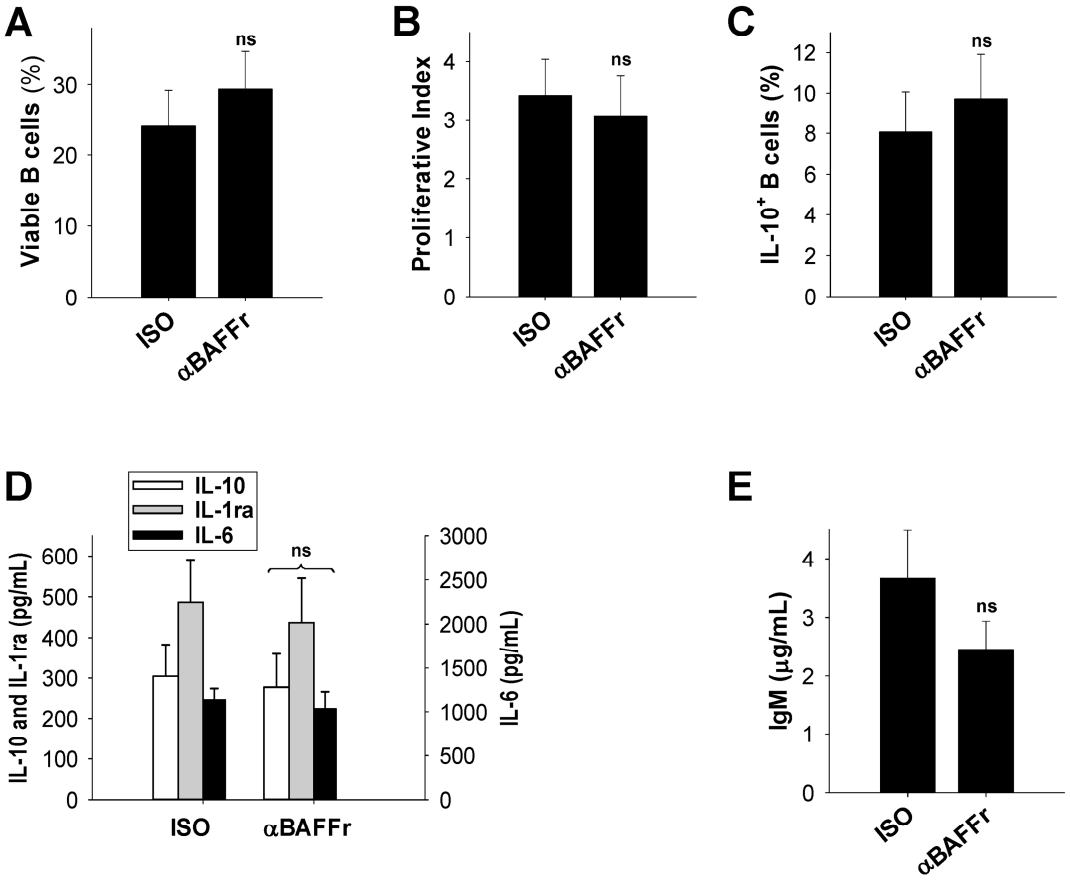

FIG E7.

The role of BAFF in CD40L$^+$ILC3 – B cell interaction

(**A-E**) B cell survival (**A**), proliferation (**B**), IL-10-producing B cell development (**C**) were analyzed by flow cytometry; cytokine (**D**) and IgM production (**E**) were measured by multiplex bead assay in cell culture supernatant of 1:3 CD40L$^+$ILC3s:B cell cocultures treated with blocking αBAFFr or isotype control (ISO) antibody. Flow cytometric and IgM measurements were performed on day 12, and cytokine measurements on day 6 (ns: $p>0.05$ vs ISO treated cocultures; n=2).

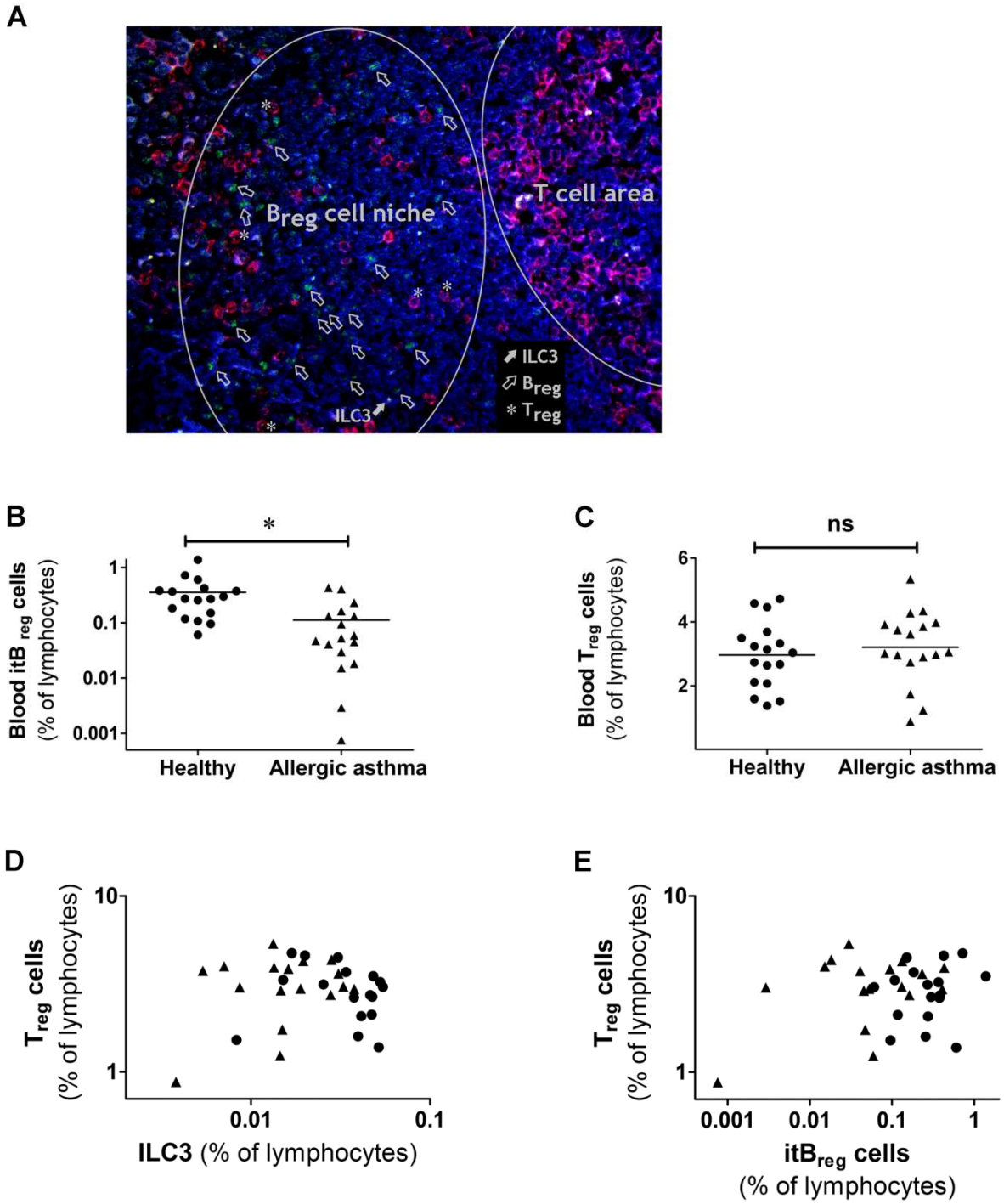

FIG E8.

Colocalization of ILC3s and IL-10^{+}B$_{reg}$ cells in the regulatory cell niches of palatine tonsils; interrelation of ILC3s itB$_{reg}$ and T$_{reg}$ cells in allergic asthma patients.

(**A**) Immunofluorescence histology of tonsils. Representative, low magnification overview picture of an interfollicular region, close to a T cell area. Colors corresponding to the same

antigens as in **Fig. 8A.** There are numerous $CD20^{+}IL\text{-}10^{+}$ B_{reg} cells (open arrows) and $CD3^{+}IL\text{-}10^{+}$ T_{reg} cells (asterisk) close to an ILC3 (filled arrow).

(**B**) Percentage of $CD19^{+}IgD^{+}IgM^{+}CD24^{high}CD38^{high}CD1d^{high}PD\text{-}L1^{+}$ itB_{reg} cells in tonsillar lymphocytes of allergic and non-allergic patients (*: $p<0.05$ Allergic asthma vs Healthy).

(**C**) Percentage of $CD3^{+}CD4^{+}IL\text{-}7R\alpha^{-}CD25^{+}$ T_{reg} cells in peripheral blood lymphocytes of allergic asthma patients and healthy controls (ns: $p>0.05$).

(**D**) Interrelation of ILC3 and T_{reg} cell percentages in peripheral blood of allergic asthma patients (triangle) and healthy controls (circle).

(**E**) Interrelation of itB_{reg} and T_{reg} cell percentages in peripheral blood of allergic asthma patients (triangle) and healthy controls (circle).

TABLE E1.

Sequences of real-time qPCR primers

mRNA	Primer	Sequences (5'-3')
EEF1A1	Forward	CCA CCT TTG GGT CGC TTT GCT GT
	Reverse	TGC CAG CTC CAG CAG CCT TCT T
RORC	Forward	CCT GGC AAA GCT GCC ACC CA
	Reverse	AGC GGC TTG GAC CAC GAT GG
IL15	Forward	TCT GAT CAT CCT AGC AAA CAA CAG
	Reverse	CCA GTT CCT CAC ATT CTT TGC AT
GATA3	Forward	GCG GGC TCT ATC ACA AAA TGA
	Reverse	GCT CTC CTG GCT GCA GAC AGC
TBX21	Forward	GAT GCG CCA GGA AGT TTC AT
	Reverse	GCA CAA TCA TCT GGG TCA CAT T
GZMB	Forward	TTC CTT TAA GGG GGA CTC TGG
	Reverse	GAG GCA TGC CAT TGT TTC GT
PRF1	Forward	TGA TGC CAC CAT TCC AGG AG
	Reverse	GAG AAG GAT GCC CAG GAG GA
CD40LG	Forward	AAG CCA GTT TGA AGG CTT TGT
	Reverse	GAG GAT TCT GAT CAC CTT TTT GCA T